Chem Soc Rev

REVIEW ARTICLE

Graphene *via* sonication assisted liquid-phase exfoliation†

Cite this: *Chem. Soc. Rev.*, 2014, **43**, 381

Artur Ciesielski and Paolo Samorì*

Graphene, the 2D form of carbon based material existing as a single layer of atoms arranged in a honeycomb lattice, has set the science and technology sectors alight with interest in the last decade in view of its astounding electrical and thermal properties, combined with its mechanical stiffness, strength and elasticity. Two distinct strategies have been undertaken for graphene production, *i.e.* the bottom-up and the top-down. The former relies on the generation of graphene from suitably designed molecular building blocks undergoing chemical reaction to form covalently linked 2D networks. The latter occurs *via* exfoliation of graphite into graphene. Bottom-up techniques, based on the organic syntheses starting from small molecular modules, when performed in liquid media, are both size limited, because macromolecules become more and more insoluble with increasing size, and suffer from the occurrence of side reactions with increasing molecular weight. Because of these reasons such a synthesis has been performed more and more on a solid (ideally catalytically active) surface. Substrate-based growth of single layers can be done also by chemical vapor deposition (CVD) or *via* reduction of silicon carbide, which unfortunately relies on the ability to follow a narrow thermodynamic path. Top-down approaches can be accomplished under different environmental conditions. Alongside the mechanical cleavage based on the scotch tape approach, liquid-phase exfoliation (LPE) methods are becoming more and more interesting because they are extremely versatile, potentially up-scalable, and can be used to deposit graphene in a variety of environments and on different substrates not available using mechanical cleavage or growth methods. Interestingly, LPE can be applied to produce different layered systems exhibiting different compositions such as BN, MoS_2, WS_2, $NbSe_2$, and TaS_2, thereby enabling the tuning of numerous physico-chemical properties of the material. Furthermore, LPE can be employed to produce graphene-based composites or films, which are key components for many applications, such as thin-film transistors, conductive transparent electrodes for indium tin oxide replacement, *e.g.* in light-emitting diodes, or photovoltaics. In this review, we highlight the recent progress that has led to successful production of high quality graphene by means of LPE of graphite. In particular, we discuss the mechanisms of exfoliation and methods that are employed for graphene characterization. We then describe a variety of successful liquid-phase exfoliation methods by categorizing them into two major classes, *i.e.* surfactant-free and surfactant-assisted LPE. Furthermore, exfoliation in aqueous and organic solutions is presented and discussed separately.

Received 27th June 2013

DOI: 10.1039/c3cs60217f

www.rsc.org/csr

Introduction

In the last decade graphene has emerged as an exciting new material, with potential to impact many areas of science and technology.[1–8] However, it is fair to note that research in this field started already in 1840s,[9] when the intercalation compounds of graphite were first reported. A good understanding of their structures was obtained in the early 1930s with the introduction of X-ray diffraction techniques. Despite systematic studies of their physical properties that began in the late 1940s, only recently the research on graphite intercalation compounds has become a field of intense activity.[10] In 1947,[11] a series of theoretical analyses suggested that isolated[12] graphene layers can exhibit extraordinary electrical properties (*e.g.* being 100 times more conducting in-plane than between planes). Nearly 60 years later, these predictions were proven to be correct, and the isolated layers of graphite were found to display other remarkable properties, such as high charge carrier mobility ($>2 \times 10^5$ cm^2 V^{-1} s^{-1} at an electron density of 2×10^{11} cm^{-2}),[13–16] very high thermal conductivity (over 3000 W mK^{-1}),[17] exceptional Young modulus values (>0.5–1 TPa), and large spring constants (1–5 N m^{-1}).[18–20] Furthermore, its high surface area, theoretically predicted as being >2500 m^2 g^{-1}[21] and experimentally measured to be 400–700 m^2 g^{-1},[5,22] has also made graphene an attractive

Nanochemistry Laboratory, ISIS & icFRC, Université de Strasbourg & CNRS, 8 allée Gaspard Monge, 67000 Strasbourg, France. E-mail: samori@unistra.fr

† Dedicated to Professor Maurizio Prato on the occasion of his 60th birthday.

material for many applications, including gas[23–25] and energy[22] storage, micro- and optoelectronics,[26–29] energy conversion,[22] as well as in catalysis[30] and biological labeling.[31] Interestingly it is fully impermeable to any gases.[32] Numerous other possible technological applications of graphene, *e.g.* in photonics and flexible electronics, ranging from solar cells[33] and light-emitting devices[34] to touch screens,[35] photodetectors,[36–39] ultrafast lasers,[40,41] spin valves,[42,43] *etc.*, are also being explored.

Graphene can be obtained in the form of very high quality sheets produced in limited quantities by chemical vapor growth,[44,45] annealing SiC substrates,[46] and building up graphene from molecular building blocks[47,48] (bottom-up). Alternatively, defect-free sheets can be produced by micromechanical cleavage,[2] ball-milling of graphite,[49] and exfoliating graphite towards graphene[50–52] (top-down). In particular, graphite can be exfoliated in liquid environments by exploiting ultrasound to extract individual layers. While excellent reviews have been published on the production and processing of graphene, these reports are either very general and discuss a variety of graphene production methods without providing much details on them,[12,53] or do not unravel the graphite exfoliation process from the chemistry viewpoint,[51] in particular the one emerging upon addition of surfactants/intercalating agents. All these issues prompted us to organize this review as a summary of the recent progress in the liquid-phase exfoliation of "pristine" graphite by exploiting a method relying on ultrasonication. Please note that this review is not intended to be exhaustive and we apologize to the authors whose work is not discussed below.

Interestingly, the majority of studies on *chemistry of graphene* do not involve "pristine" graphene, but rather carbon materials produced upon reduction of graphene oxide (GO) because of the proven scalability and ease of these methods. In general, GO is synthesized by either the Brodie,[54] Staudenmaier,[55] or Hummers method,[56] or some variation of these methods. All three methods involve oxidation of graphite to various levels. Brodie and Staudenmaier used a combination of potassium chlorate ($KClO_3$) with nitric acid (HNO_3) to oxidize graphite, and the Hummers method involves treatment of graphite with potassium permanganate ($KMnO_4$) and sulfuric acid (H_2SO_4). One of the *pros* of GO is undoubtedly that it is easily processible in liquid media such as water.[57–59] Moreover all the different functional groups that are exposed on GO, including hydroxyl, epoxy, carbonyl and carboxyl groups, can be used to covalently and non-covalently attach functional units to this 2D scaffold, thereby changing its physical and chemical properties.[60–65] However, because of heteroatomic contamination and/or topographical defects, it is misleading to refer to such materials as graphene. Furthermore, GO suffers from some important drawbacks. Because of the presence of oxides, *i.e.* epoxy bridges, hydroxyl groups and carboxyl groups, GO is a poor electrical conductor.[66] While the oxides can be removed by reduction resulting in reduced graphene oxide (RGO),[57,66–70] this adds yet another step in the processing procedure. The greatest problem is that reduction cannot remove all structural defects introduced by the oxidation process.[66,71–75] These defects disrupt the band structure and completely degrade the electronic properties that make graphene unique.

1. Sonication assisted liquid-phase exfoliation (LPE)

Graphite can be successfully exfoliated in liquid environments by exploiting ultrasound to extract individual layers. The liquid-phase exfoliation (LPE) (Fig. 1) process typically involves three steps: (1) dispersion of graphite in a solvent, (2) exfoliation, and (3)

Artur Ciesielski

Artur Ciesielski earned a Diploma in Chemistry at the Adam Mickiewicz University (Poland) in 2007, and received his PhD at the Université de Strasbourg (France) in 2010. From there, he became a postdoctoral associate, working for Paolo Samorì at the Institut de Science et d'Ingénierie Supramoléculaires of Université de Strasbourg. His current research interests include the design of supramolecular systems, self-assembly of nanopatterns and production of high-quality graphene via liquid-phase exfoliation of graphite by using supramolecular approaches.

Paolo Samorì

Paolo Samorì is Distinguished Professor (PRCE) and director of the Institut de Science et d'Ingénierie Supramoléculaires (ISIS) of the Université de Strasbourg (UdS) & CNRS where he is also head of the Nanochemistry Laboratory. He is also a Fellow of the Royal Society of Chemistry (FRSC) and junior member of the Institut Universitaire de France (IUF). He received his PhD in Chemistry from the Humboldt University Berlin (Prof. J. P. Rabe). Previously he was a research scientist at Istituto per la Sintesi Organica e la Fotoreattività of the Consiglio Nazionale delle Ricerche of Bologna. He has published >180 papers on applications of scanning probe microscopy beyond imaging, hierarchical self-assembly of hybrid architectures at surfaces, supramolecular electronics, and the fabrication of organic-based nanodevices.

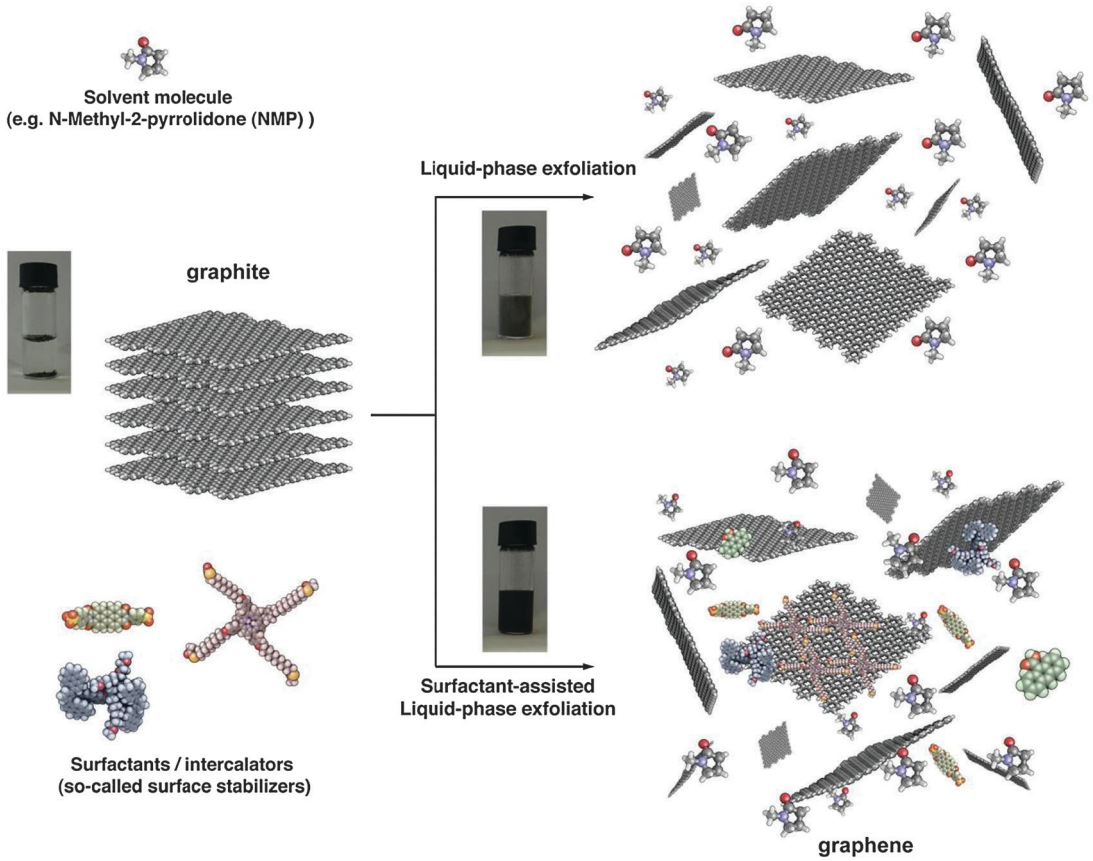

Fig. 1 Schematic representation of the liquid-phase exfoliation process of graphite in the absence (top-right) and presence (bottom-right) of surfactant molecules.

purification. Graphene flakes can be produced by surfactant-free exfoliation of graphite *via* chemical wet dispersion, followed by ultrasonication in organic solvents.[76–84] During ultrasonication, shear forces and cavitation,[85] *i.e.* the growth and collapse of the micrometer-sized bubbles or voids in liquids due to pressure fluctuations, act on the bulk material and induce exfoliation. After exfoliation, the solvent–graphene interaction needs to balance the inter-sheet attractive forces. Solvents ideal to disperse graphene are those that minimize the interfacial tension [mN m^{-1}] between the liquid and graphene flakes, *i.e.* the force that minimizes the area of the surfaces in contact.[86] Different solvents have been used for graphite exfoliation, and will be discussed in Section 1.2.

1.1 Characterization methods

The LPE yield can be described by different analytical approaches. The yield by weight is defined as the ratio between the weight of dispersed graphitic material and that of the starting graphite flakes. The yield by single-layered graphene (SLG) percentage is defined as the ratio between the number of SLG and the total number of graphitic flakes in the dispersion. The yield by SLG weight is expressed as the ratio between the total mass of dispersed SLG and the total mass of all dispersed flakes. The yield by weight does not give information on the amount of SLG, but only on the total amount of graphitic material. Yields by SLG percentage and weight are more suitable to quantify the amount of dispersed SLGs.

In order to determine exfoliation yields it is necessary to characterize exfoliated graphitic material providing both qualitative and quantitative information. An ideal graphene characterization tool should be fast and non-destructive, offer high resolution, give structural and electronic information, and be applicable at both laboratory and mass-production scales. In particular, the estimation of the concentration c [g L^{-1}] of dispersed graphitic material is important. c is usually determined *via* optical absorption spectroscopy (OAS),[76] by exploiting the Beer–Lambert Law: $A = \alpha c l$, where A is the absorbance, l [m] is the length of the optical path, and α [L g^{-1} m^{-1}] is the absorption coefficient. α can be experimentally determined by filtering a known volume of dispersion, *e.g. via* vacuum filtration, onto a filter of known mass,[76] and measuring the resulting mass using a microbalance.

The number of graphene layers (N), *i.e.* the thickness of exfoliated graphitic material, is usually determined *via* transmission electron microscopy (TEM) and atomic force microscopy (AFM) (Fig. 2). In TEM, N can be counted both by analyzing the edges[87] of the flakes and by using electron diffraction patterns. AFM enables the estimation of N by measuring the height of the deposited flakes and dividing it by the graphite interlayer distance. However, the estimation of

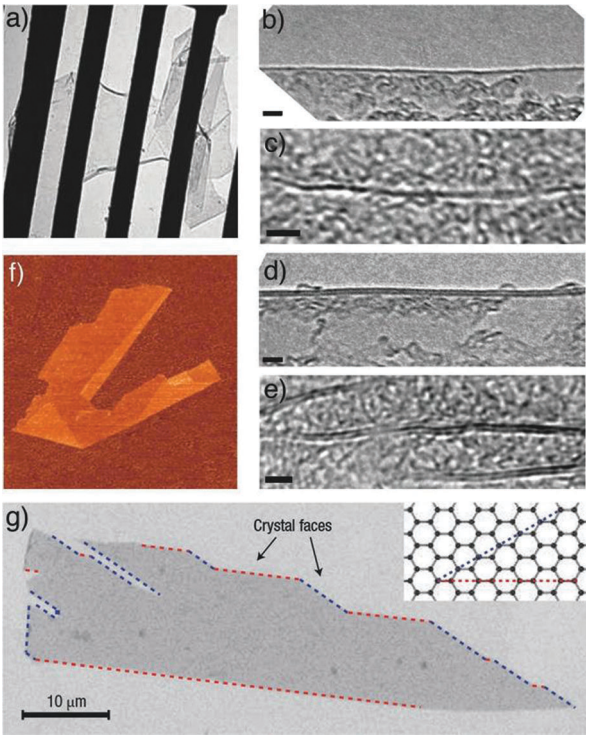

Fig. 2 (a) A graphene sheet freely suspended on a micrometre-sized metallic scaffold. The TEM image is adapted from ref. 89 with permission from the Nature Publishing Group; (b–e) high-resolution images of a folded edge of a single layer (a) and a wrinkle within the layer (c); folded edge of a two layer (d), and internal foldings of the two layer (e), adapted from ref. 87 with permission from the American Physical Society; (f) graphene visualized using an AFM (adapted from ref. 2 with permission from the National Academy of Sciences). The folded region exhibiting a relative height of ≈4 Å clearly indicates that it is a single layer; (g) scanning electron micrograph of a relatively large graphene crystal, which shows that most of the crystal's faces are zig-zag and arm-chair edges as indicated by blue and red lines and illustrated in the inset (adapted from ref. 3 with permission from the Nature Publishing Group).

the height of a single layer of graphene *via* AFM depends on the substrate and on the environmental conditions such as relative humidity. Indeed, on SiO_2, a single-layer graphene (SLG) can appear to have a height of ~1 nm,[2] while on mica it amounts to ~0.4 nm.[88]

The number of graphene layers (N) in a sample can be determined by elastic light scattering (Rayleigh) spectroscopy,[90,91] although this approach only works for exfoliated samples on optimized substrates and does not provide other structural or electronic information. On the other hand, Raman spectroscopy[92,93] can be applied to all graphene samples.[87,94] Moreover, it is able to identify unwanted by-products, structural damage, functional groups, chemical modifications and electronic perturbations introduced during the preparation, processing or placement of graphene.[53] As a result, a Raman spectrum is an invaluable tool for quality control, and for comparing samples used by different research groups.

In the past six years, there has been a significant step forward in the understanding of Raman spectroscopy in graphene, fuelled by new results on doping,[95–100] edges,[101–105]

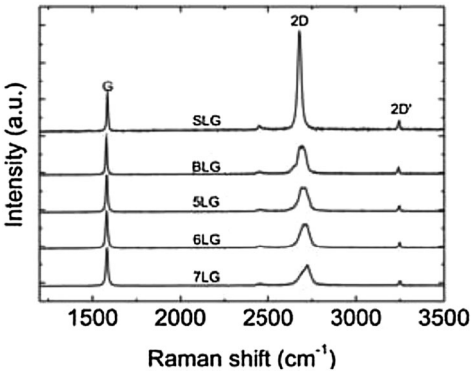

Fig. 3 Evolution of Raman spectra with the number of graphene layers. The spectra are normalized to have the same G peak intensity. Spectra adapted from ref. 87 with permission from the American Physical Society.

oxidation,[106] and electrical mobility.[107,108] Typically, Raman spectroscopy is used for the determination of exfoliation yield and to confirm the results obtained with TEM and/or AFM (Fig. 3).

1.2 Solvent

The distance between stacked parallel graphene layers in bulk graphite amounts to 3.35 Å. Although the van der Waals attractions among adjacent layers are weak enough to let them slide on each other in the direction perpendicular to the *c*-axis, the attraction is strong enough to make complete exfoliation into individual layers challenging. The first attempt by Brodie to produce single-layer graphene sheets by exfoliation dates as far back as 1859.[109] Since then, many unsuccessful attempts have been made to come up with solutions for the large-scale production of graphene.[110–113] Successful exfoliation requires the overcoming of the van der Waals attractions between the adjacent layers. One of the most effective and straightforward methods to reduce the strength of the van der Waals attractions is liquid immersion, where the potential energy between adjacent layers is contributed by the dispersive London interactions, which in the presence of a solvent are significantly reduced with respect to vacuum. In the past decades, it has been found that interfacial tension plays a key role when a solid surface is immersed in a liquid medium.[86] If the interfacial tension between solid and liquid is high, there is poor dispersibility of the solid in the liquid.[86] In the case of graphitic flakes in solution, if the interfacial tension is high, the flakes tend to adhere to each other and the work of cohesion between them is high (*i.e.* the energy per unit area required to separate two flat surfaces from contact),[86] hindering their dispersion in the liquid. Solvents with surface tension (*viz.* the property of the surface of a liquid that allows it to resist an external force, due to the cohesive nature of its molecules) $\gamma \sim 40$ mJ m^{-2}[76] are *the best* solvents for the dispersion of graphene and graphitic flakes, since they minimize the interfacial tension between solvent and graphene. Unfortunately, the majority of solvents with $\gamma \sim 40$ mJ m^{-2} such as *N*-methyl-2-pyrrolidone (NMP – 40 mJ m^{-2}), *N*,*N*-dimethylformamide (DMF – 37.1 mJ m^{-2}), and *ortho*-dichlorobenzene (*o*-DCB – 37 mJ m^{-2}) (Fig. 4)

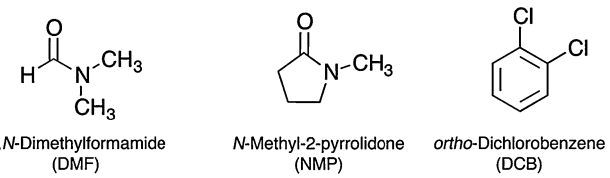

Fig. 4 Chemical structure of common solvents used as liquid media in the graphite exfoliation process.

[see ref. 76 for a complete list of solvents tested as exfoliation media] have some disadvantages, *e.g.* NMP is an eye irritant and may be toxic to the reproductive organs,[114] while DMF may have toxic effects on multiple organs.[115] Therefore, the search for additional solvents in this context is highly recommended in order to strengthen the universal character of this genuine approach by providing more choices.

In 2009 Bourlinos[77] and co-workers proposed solvents belonging to a peculiar class of perfluorinated aromatic molecules and tested their efficiency in exfoliating graphite; to this end perfluorinated analogues of hydrocarbon solvents, *i.e.* benzene, toluene, nitrobenzene, and pyridine, were employed (Fig. 5).

Graphite fine powder was suspended by relatively short sonication (1 h) in a series of perfluorinated aromatic solvents yielding moderately dark-gray colloidal dispersions. Depending on the solvent, the concentrations of the dispersions ranged between 0.05 and 0.1 mg mL^{-1}, whereas the solubilization yield spanned from 1% to 2%. The performance of each solvent sorted by increasing order was as follows: octafluorotoluene $\sim$ pentafluoropyridine $<$ hexafluorobenzene $<$ pentafluorobenzonitrile. Hence, pentafluorobenzonitrile provided the highest colloidal concentration and solubilization yield (0.1 mg mL^{-1}, 2%) with octafluorotoluene and pentafluoropyridine equally exhibiting the poorest function (0.05 mg mL^{-1}, 1%). Hexafluorobenzene displayed an intermediate efficacy within this series, as testified by a concentration of 0.07–0.08 mg mL^{-1} and a solubilization yield of 1.5%. Raman and IR spectroscopy provided evidence for the virtual non-oxidization of the as-dispersed graphitic solids. AFM analysis of average flake thickness was estimated to range between 0.6 and 2.0 nm, suggesting the existence of a few-layer thick graphene (FLG) nanosheets.

Noteworthy, in 2011 Mariani and co-workers[81] suggested that graphene could be obtained by sonication of graphite powder in an ionic liquid, namely 1-hexyl-3-methyl-imidazolium hexafluorophosphate (HMIH). Unfortunately, while the graphene concentration was estimated as being as high as 5.33 mg mL^{-1}, the AFM analysis showed the presence of 2 nm thick graphite-like flakes, highlighting a low exfoliation yield.

These above solvents have surface tensions close to 40 mJ m^{-2}, and are suitable for the direct exfoliation of graphene. However, their high boiling points (NMP 203 °C, *o*-DCB 181 °C, DMF 154 °C) limit their viability for real manipulation, in particular in organic electronics. Especially, it is of paramount importance to extract the conductivity and field-effect mobility in field-effect transistor (FET) devices if solution processed graphene flakes are to be harnessed in real electronics applications given that the mobility governs the device's frequency response. Furthermore, high-mobility devices are absolutely desirable in electronics because they can work at moderately low-voltage conditions, *i.e.* they can be integrated in low-power and portable circuitry. Some attempts of using liquid-phase exfoliated graphene have been made, *e.g.* field-effect mobility measured on liquid-phase exfoliated graphene-based FETs prepared by inkjet printing was found to be as high as 95 $cm^2 V^{-1} s^{-1}$.[64]

In general, sample preparation for electrical measurements requires complete removal of solvents, since the presence of remaining solvent can greatly impact the device performance. Thus, dispersion of graphene in low boiling solvents is preferable. On the other hand, most low boiling solvents, *e.g.* water, ethanol, and chloroform, have a surface tension (72.8 mJ m^{-2}, 22.1 mJ m^{-2} and 27.5 mJ m^{-2}, respectively) unsuitable for the direct exfoliation of graphene.

Hitherto several attempts of producing graphene by LPE in low boiling solvents have been reported. For example, in 2009 Hou[63] and co-workers anticipated a solvothermal-assisted

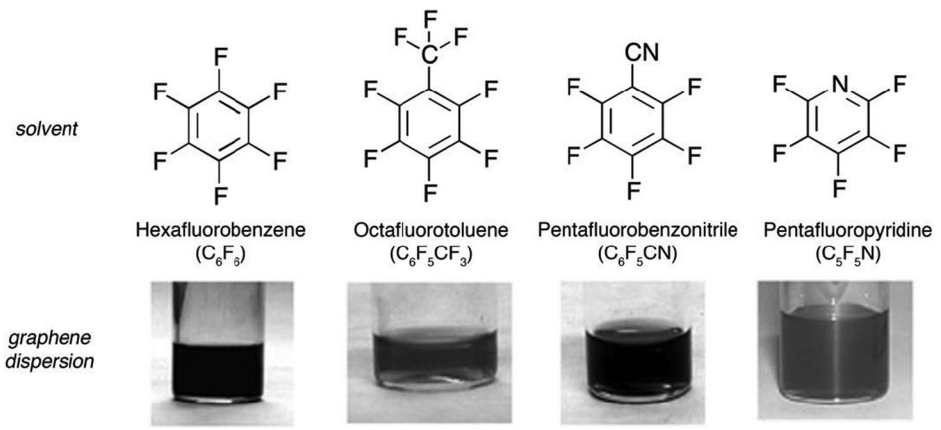

Fig. 5 Colloidal dispersions obtained after liquid-phase exfoliation of graphite using perfluorinated aromatic solvents. Image adapted from ref. 77 with permission from Wiley-VCH.

exfoliation process of expanded graphite (EG) in a highly polar organic solvent, *i.e.* acetonitrile. It has been proposed that the dipole-induced dipole interactions between graphene and acetonitrile facilitate the exfoliation and dispersion of graphene. The solvothermal-assisted exfoliation process resulted in yield of *ca.* 10 wt% graphene.

Recently, Feringa and co-workers[80] reported that dispersion of graphene could be obtained in ethanol using solvent exchange from NMP, which enables broader application of dispersed graphene. Approximately 200 mg of graphite in 200 ml NMP was sonicated for 2 h and centrifuged at 4000 rpm for 30 min to remove large particles. The supernatant of graphene in NMP was decanted and then filtered through a poly-tetrafluoroethylene (PTFE) membrane. The obtained filter cake was dispersed in ethanol with mild sonication and filtered again. This process was repeated five times and finally the filter cake was redispersed in ethanol. This suspension was centrifuged at 1000 rpm for 30 min, the supernatant was decanted and further sonicated for several minutes to give the required homogeneous graphene dispersion in ethanol. The repeated washing steps yield a stable dispersion of graphene in ethanol (0.04 mg mL^{-1}) containing *ca.* 0.3 vol% NMP. Films prepared from such dispersions show good conductivity (1130 S m^{-1}). Noteworthy, over one week, the sample shows 20% sedimentation.

1.3 Sonication time

Since the first successful exfoliation of graphene in an organic solvent such as NMP in 2008,[76] improvements in concentrations of graphene dispersions have been achieved, *e.g.* by using drastically longer sonication times ($\sim$500 h–2 mg mL^{-1})[79] (Fig. 6). Such a time consuming approach requires high energy; in addition, as previously observed for nanotubes, with the increasing sonication time, the size of the flakes is severely reduced,[116] being a critical parameter for several applications.

In addition to the reduced flake size, long sonication of graphite can also affect the quality of graphene. The analysis of Raman spectra can provide information on the number and position of broken-conjugation areas in graphene, so-called graphene atomic- or point-defects, which can affect the electronic properties of graphene. Typically, sonication of graphite is considered as a nondestructive process; therefore defects are predominantly located at the edges of the graphene flakes, and the basal plane of the flakes is relatively defect free.[117] However, in some cases the small size of the flakes precludes spatial mapping of the defects and hence identification of their location on the edge or in the basal plane.

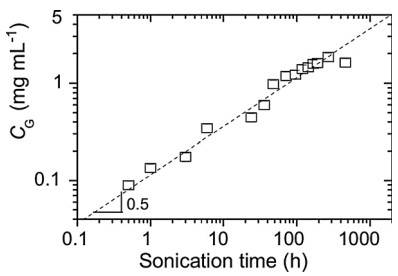

Fig. 6 Concentration of graphene in NMP after centrifugation as a function of sonication time. Adapted from ref. 79 with permission from Wiley-VCH.

1.4 Centrifugation

The majority of the material in the dispersion after sonication is composed of thick graphite-like flakes, which can be removed by different strategies based on differential ultracentrifugation (sedimentation-based separation, SBS)[62] in a uniform medium or in a density gradient medium (DGM).[118] The SBS process separates particles on the basis of their sedimentation degree in response to centrifugal force acting on them.[62]

It is worth taking into account that liquid-phase exfoliation of graphite generally results in flakes with lateral size of one micrometer or less, hence being too small for many applications such as mechanical reinforcement of composites.[119] To address this issue, Coleman and co-workers described a method to separate an existing dispersion with a mean flake size length of $\approx$1 μm into fractions, each with different mean flake size.[84] The initial graphene dispersion in NMP was centrifuged at a high centrifugation rate, separating the small flakes in the supernatant from large flakes in the sediment. Redispersion of the sediment, followed by successive centrifugation, separation and redispersion cycles resulted in separation of flakes by size (Fig. 7a). Such a procedure resulted in a range of dispersions with the mean flake length varying from 1 μm for the highest centrifugation rate to 3.5 μm for the sample whose final centrifugation rate was 500 rpm. By TEM analysis of various samples, it has been found that flakes obtained with 3000 rpm centrifugation speed are much smaller than the 500 rpm ones (Fig. 7b). Noteworthy, by decreasing the centrifugation speed increased number of graphene layers per flake was noted (Fig. 7c).

2. Surfactant assisted exfoliation

The use of small organic molecules such as surfactants, can promote the exfoliation of graphite into graphene, in particular when such a molecule has a high energy of adsorption on the basal plane of graphene, and in particular being higher than the one of the solvent molecule interacting with the graphene. The use of surfactants can also stabilize exfoliated graphene in water and organic solvents, where the ζ potential of the surfactant-coated graphene nanosheets controls the dispersed concentration.[117]

2.1 Aqueous dispersions

Water is a natural choice because of its non-toxicity which opens perspective for the formation of biocompatible graphene based materials for biomedical applications.[120] However, the exfoliation of graphene in water is particularly challenging due to the hydrophobic nature of the sheets. Such a challenge can be overcome by using surfactants which allow exfoliated sheets to remain suspended.[77,102,117,121–136] In particular polycyclic

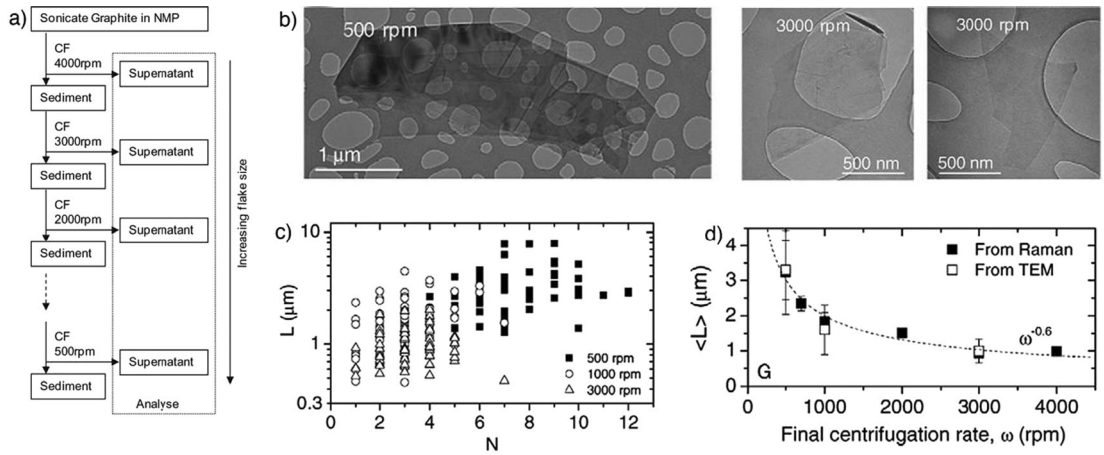

Fig. 7 (a) Schematic representation of the flake separation process; (b) TEM images of flakes prepared at final centrifugation rates of 5000 rpm and 3000 rpm; (c) individual flake length plotted *versus* estimated flake thickness (number of monolayers, *N*) for dispersions with final centrifugation rates of 500, 1000 and 3000 rpm; (d) mean flake size as measured from TEM images. Adapted from ref. 84 with permission from Elsevier.

aromatic hydrocarbons (PAHs)[137–141] show promise in this regard due to their π–π stacking interactions with graphene.[142,143]

2.1.1 Pyrenes. Pyrene derivatives have been used by various groups to stabilize carbon nanotube and graphene dispersions.[144] Adsorption of these compounds onto the graphene surface occurs through π–π interactions between the planar π-conjugated surfaces, by reducing the surface free energy of the dispersion. In these interactions both aromatic planar surfaces share the electrons of π-orbitals through a non-covalent bond. Fig. 8 portrays the chemical formulae of various pyrene derivatives used as surfactant additives in LPE of graphite. In these representative molecules, different functional polar or apolar groups are decorating the pyrene aromatic core.

For example, He and co-workers exfoliated single layers of graphene into an aqueous dispersion by using 1,3,6,8-pyrenetetrasulfonic acid tetrasodium salt (Py–$(SO_3)_4$) (see Fig. 8) and aminomethylpyrene (Py–Me–NH_2) to fabricate transparent conductive films.[145] However, neither the graphene yield nor the dispersion effectiveness and stability were examined, and aggregates likely remained in these dispersions besides final products. In other attempts to stabilize graphene through π–π stacking, Shi *et al.*,[146] Müllen *et al.*,[123] and Honma *et al.*[126] used pyrenebutyrate and pyrenesulfonic acid sodium salt (Py–SAH) to stabilize graphene in water for use in electrochemical, solar cell, and composite applications.

In a different study, a variety of pyrenes were employed by Green and co-workers to test their ability to obtain high exfoliation yield and dispersion of graphene in water.[134] Among all investigated pyrene derivatives, *i.e.* pyrene (Py), 1-aminopyrene (Py–NH_2), 1-aminomethyl pyrene (Py–Me–NH_2), 1-pyrenecarboxylic acid (Py–CA), 1-pyrenebutyric acid (PyBA), 1-pyrenebutanol (PyBOH), 1-pyrenesulfonic acid hydrate (PySAH), 1-pyrenesulfonic acid sodium salt (Py–SO_3) and 1,3,6,8-pyrenetetrasulfonic tetra acid tetra sodium salt (Py–$(SO_3)_4$), the Py–SO_3 was found to be the most effective one, yielding graphene final concentrations as high as 0.8–1 mg mL^{-1} (Fig. 9a). To confirm the presence of single- or few-layer stabilized graphene in the dispersions, the Py–SO_3-stabilized graphene samples were characterized by HRTEM. A commonly used method to quantify the number of layers in graphene is by counting the number of folds at the edge of a graphene sheet in HRTEM images. A HRTEM image of a Py–SO_3-stabilized graphene sheet is shown in Fig. 9b. The edge count of the graphene sheets reveals that the Py–SO_3-stabilized graphene is 2–4 layers thick, as commonly observed in sonicated and centrifuged samples.

By using a similar approach to that using pyrene derivatives, Palermo and co-workers[135] went one step further into the thermodynamics of liquid-phase exfoliation of graphite. The authors studied the mechanism of surface adsorption of organic pyrene dyes on graphene, and successive exfoliation in water of these dye-functionalized graphene sheets. A systematic, comparative study was performed on pyrenes functionalized with an increasing number of sulfonic groups, *i.e.* 1-pyrenesulfonic acid sodium salt (Py–SO_3), 6,8-dihydroxy-1,3-pyrenedisulfonic acid disodium salt (Py–$(OH)_2(SO_3)_2$), 8-hydroxy-1,3,6-pyrenetrisulfonic acid trisodium salt (Py–$OH(SO_3)_3$), and 1,3,6,8-pyrenetetrasulfonic acid tetrasodium salt (Py–$(SO_3)_4$). By combining experimental and modeling investigations, the correlation between graphene–pyrene interaction energy, the molecular structure and the amount of graphene flakes solubilized has been unravelled. The results obtained indicate that the molecular dipole is not important *per se*, but since it facilitates adsorption on graphene, it promotes lateral displacement of water molecules collocated between the aromatic cores of the organic dye and graphene. Additionally, the effect of charges present corresponding to –OH groups has been explored by sonicating graphite with the respective dyes at different pH. A distinct influence of pH on the total amount of suspended graphene was observed. The pH dependent absorption of dyes is portrayed in Fig. 10a.

2.1.2 Alternative surface stabilizers. Several alternative surfactants, also called surface stabilizers, have been used to promote the exfoliation of graphite in aqueous solutions, including perylene-based bolaamphiphiles[122,147] (PBBA – Fig. 11),

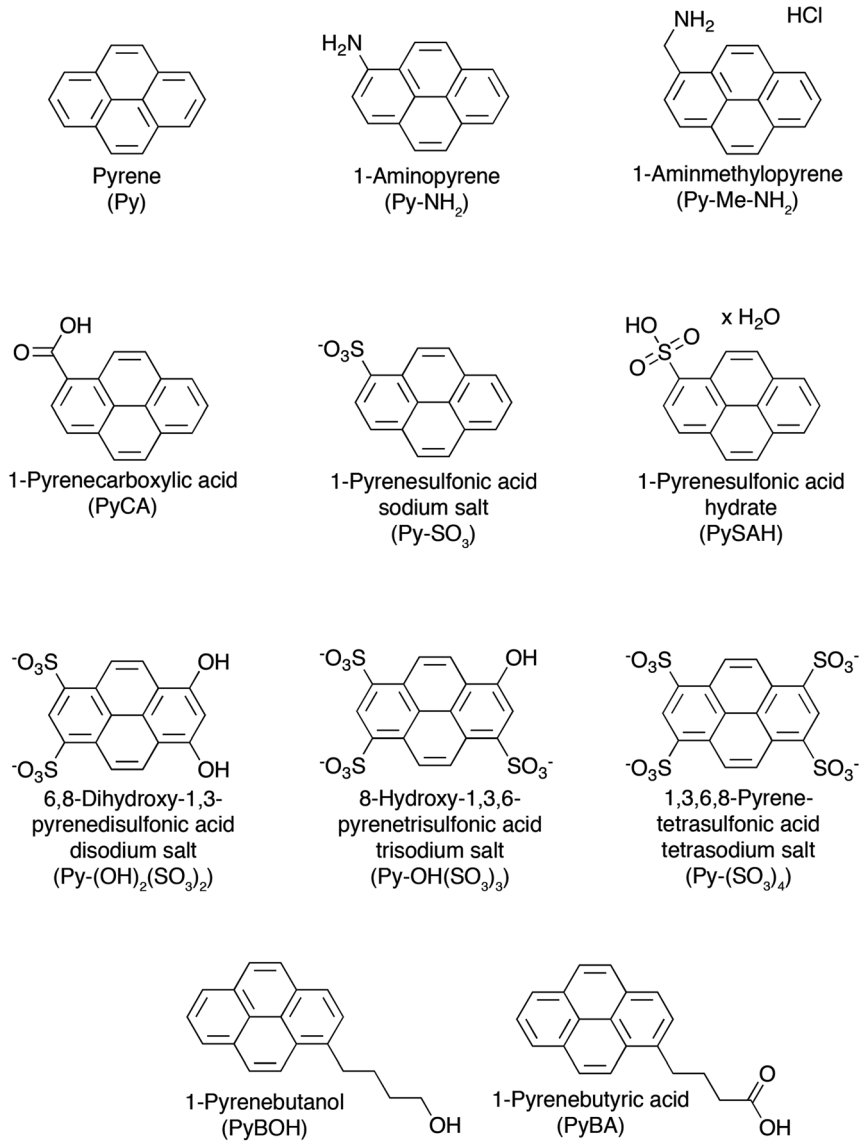

Fig. 8 Chemical structures of pyrene derivatives used as surfactants in the process of LPE of graphite towards graphene, with their names and corresponding acronyms as used in the text.

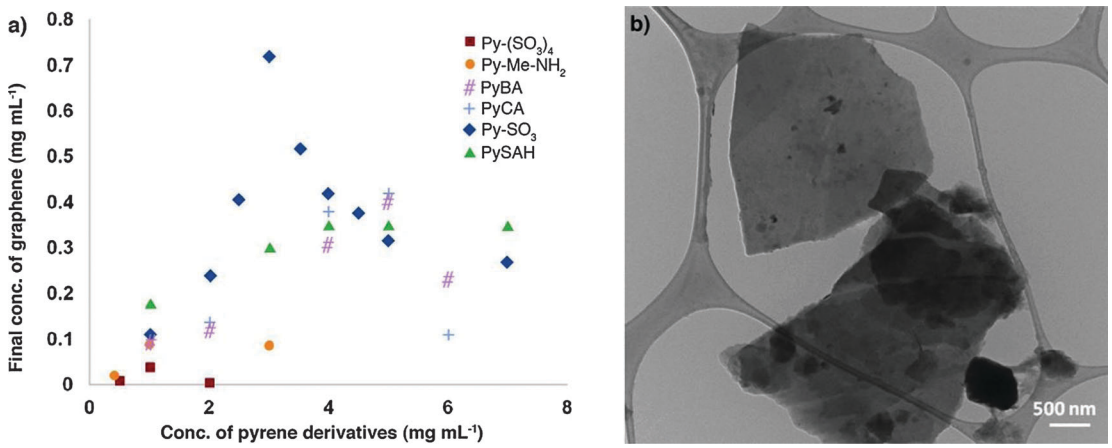

Fig. 9 (a) Final concentration of graphene for different pyrene derivatives. The initial concentration of graphite in all samples is 20 mg mL^{-1}; (b) TEM image of stabilized graphene layers in a Py–(SO_3)–graphene dispersion. The lateral size of graphene sheets is about 2–2.5 μm. Adapted from ref. 134 with permission from the American Chemical Society.

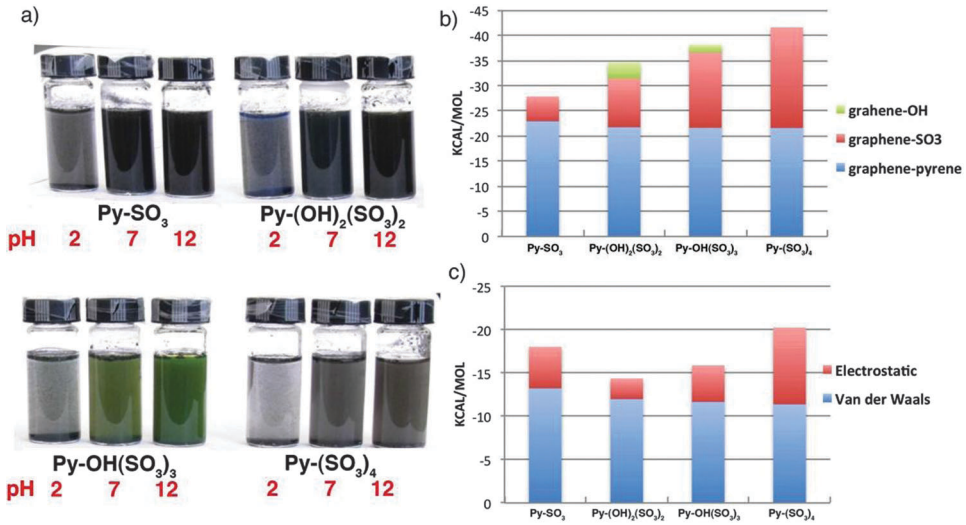

Fig. 10 (a) Image of the solutions obtained on sonicating graphite with the different pyrenes at pH = 2, 7 and 10; (b) contribution of the different components of pyrenes to the interaction energy of the molecules with graphene; (c) electrostatic and van der Waals contributions of the pyrene core of adsorbed molecules with the surrounding aqueous medium. Adapted from ref. 135 with permission from the Royal Chemical Society.

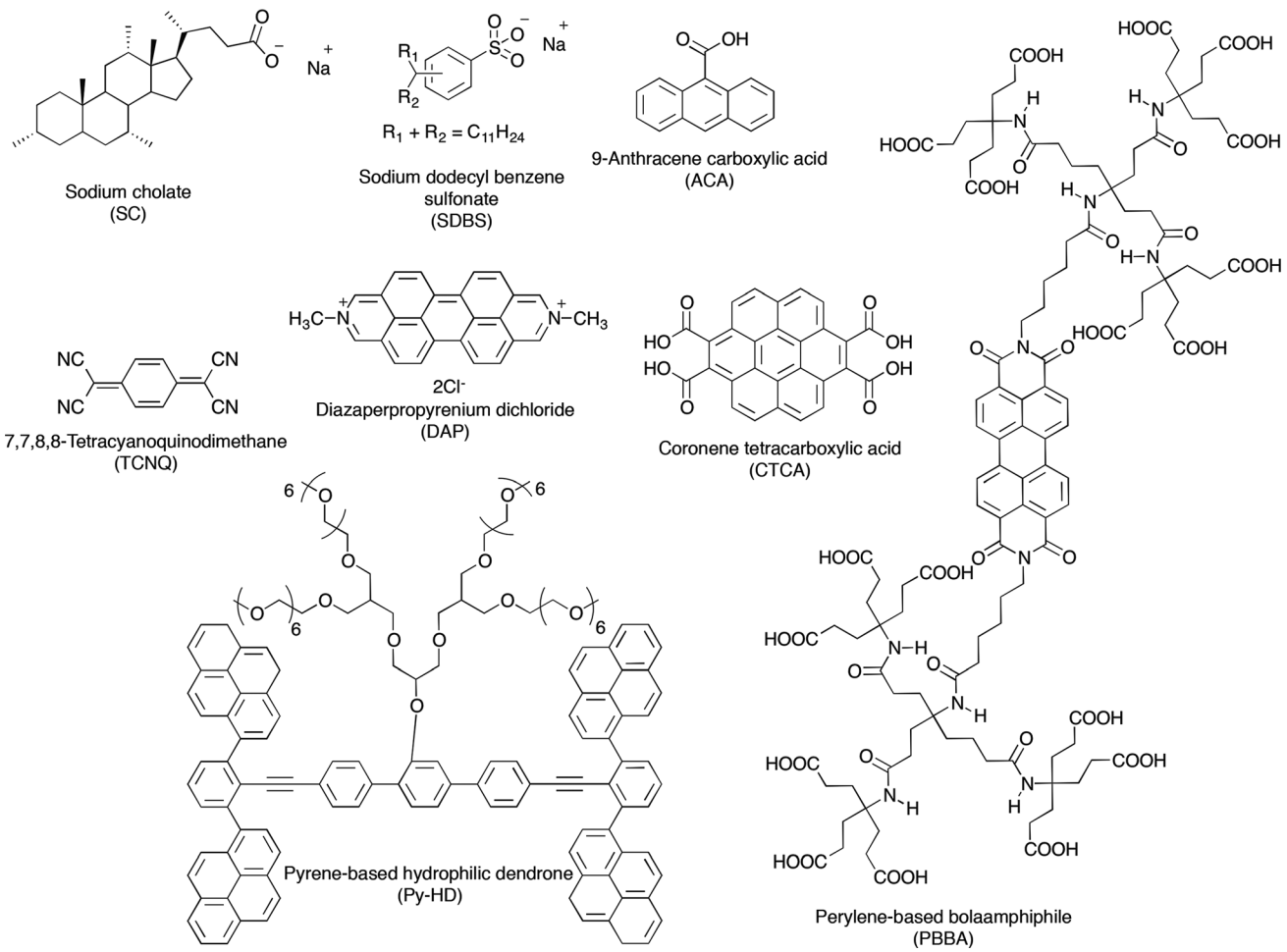

Fig. 11 Chemical structures of organic molecules used as surfactants in the process of LPE of graphite towards graphene, with their names and corresponding acronyms as used in the text.

7,7,8,8-tetracyanoquinodimethane (TCNQ),[148] coronene tetracarboxylic acids (CTCA),[125] or pyrene-based hydrophilic dendrones,[127] to name a few. In particular, graphene dispersions can be stabilized in water by the surfactant sodium cholate (SC),[129,149] at concentrations up to 0.3 mg mL^{-1}. The dispersed concentration increases with sonication time while the best quality dispersions are obtained for centrifugation rates between 500 and 2000 rpm. Detailed TEM analysis shows the flakes to consist of 1–10 stacked monolayers with up to 20% of flakes containing just one layer. The average flake consists of ~4 stacked graphene layers and has a length and width of ~1 μm and ~400 nm, respectively. These dimensions are surprisingly stable under prolonged sonication. However, the mean flake length falls from ~1 μm to ~500 nm as the centrifugation rate is increased from 500 to 5000 rpm.

Exfoliation of graphite can be also achieved by non-covalent functionalization using 9-anthracene carboxylic acid (ACA).[124] Interestingly, ACA–graphene based materials possess remarkable electronic properties, *i.e.* an ACA–graphene based ultracapacitor demonstrates a high specific capacitance value of 148 F g^{-1}.

Though the majority of the previously mentioned studies showed improved stability, only a few of them provided a quantitative investigation of the average lateral size or thickness of the sheets obtained. In fact conventional studies simply relied on a TEM analysis showing the presence of monolayers and a few-layer stacks. A quantitative insight into the effectiveness of the proposed method, in particular the choice of the surfactant, can be achieved only by an in-depth analysis of exfoliated material. In particular, Coleman and co-workers[117] demonstrated that the use of sodium dodecylbenzene sulfonate (SDBS) could be extremely successful. Statistical Raman analysis revealed a reasonable population of few-layer graphene, *e.g.* ~43% of flakes had <5 layers. More importantly, ~3% of the flakes were found to be monolayer thick. These data are illustrated in the histogram for the standard dispersion in Fig. 12. Even more importantly, the sediment remaining after centrifugation can be recycled to improve the overall yield of graphene exfoliation. Recycling the sediment results in narrowing of the flake thickness distribution, shifting it toward thinner flakes with large quantities of bilayers and trilayers; 67% of flakes observed had <5 layers.

Another effective and efficient method for the preparation of graphene by LPE in aqueous solutions was demonstrated by Stoddart, Stupp and co-workers.[136] *N*,*N*′-dimethyl-2,9-diazaperpropyrenium dichloride (DAP) molecules were used in order to stabilize exfoliated graphene sheets in water. It was found that the electrostatic repulsion between the positively charged regions present in DAP^{2+} minimizes the aggregation of graphene layers and helps in sustaining a stable dispersion of the graphene sheets in water. Photographs (Fig. 13a) of aqueous dispersions of graphite, DAP, and DAP–graphene dispersions in water under ambient and UV light offered qualitative evidence for the almost complete quenching of the strong fluorescence signature associated with solvated DAP in the presence of graphene. The thicknesses of the graphene sheets were measured by AFM, with both the AFM height image of graphene sheets and the height profile of the AFM image (Fig. 13b) revealing the thickness of the graphene sheets and the distribution of layer thickness. These observations showed that the exfoliated graphene sheets are predominantly 2 to 4 layers thick.

2.2 Organic dispersions

The use of water as an exfoliation medium is not recommended for the exploitation of graphene in electronic devices such as field-effect transistors (FETs) because the presence of residual water molecules at the interface with dielectrics can enhance charge trapping phenomena.[150] Therefore, the use of organic solvents as exfoliating media has to be explored. Despite the increasing interest in the field, the knowledge gathered about the surfactant-assisted LPE of graphite in organic solvents is still relatively poor (Fig. 14).[151–154]

A recently reported approach[153] involves the use of 1,2-distearoyl-*sn*-*glycero*-3-phosphoethanolamine-*N*-[methoxy(polyethyleneglycol)-5000] (DSPE-mPEG) molecules in combination

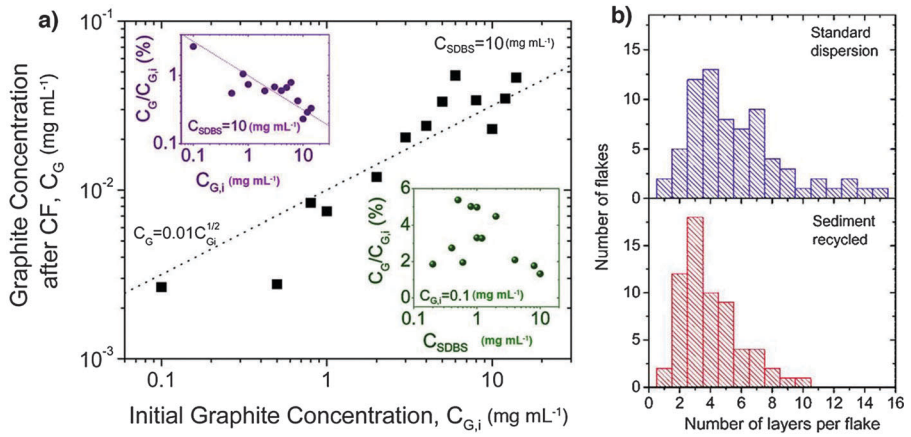

Fig. 12 (a) Graphite concentration after centrifugation as a function of starting graphite concentration (C_{SDBS} = 10 mg mL^{-1}). Upper inset: the same data represented as the fraction of graphite remaining after centrifugation. Lower inset: fraction of graphite after centrifugation as a function of SDBS concentration ($C_{G,i}$ = 0.1 mg mL^{-1}); (b) histogram of number of layers per flake for dispersions from original sieved graphite and from recycled sediment. Adapted from ref. 117 with permission from the American Chemical Society.

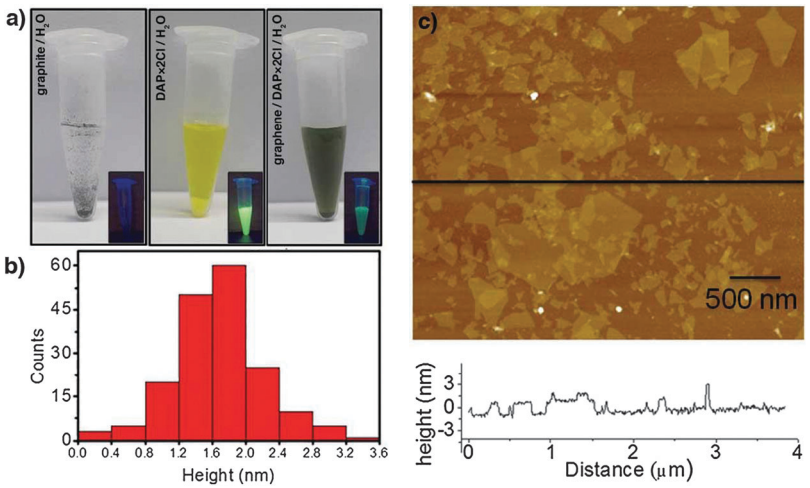

Fig. 13 (a) Photographs of graphite, DAP·2Cl, and DAP·2Cl/graphene in water under ambient light and under UV light (insets); (b) probability of occurrence of graphene layers with various thicknesses calculated by measuring the thickness of the graphene sheets using the AFM height image; (c) AFM height image of DAP·2Cl/graphene, along with the height profile. Adapted from ref. 136 with permission from Wiley VCH.

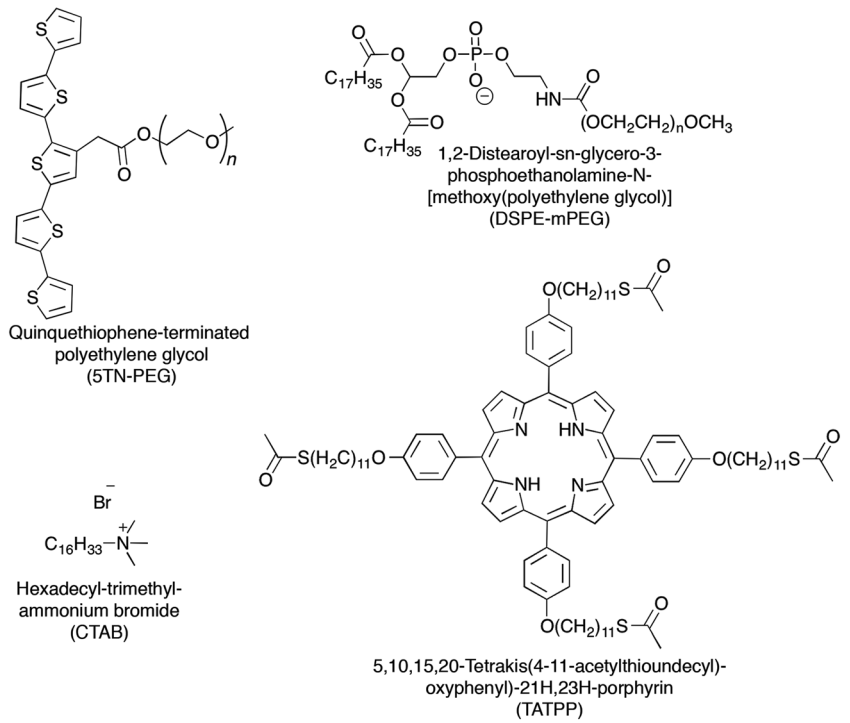

Fig. 14 Chemical structures of organic molecules used as surfactants in the process of LPE of graphite towards graphene in organic solvents, with their names and corresponding acronyms as used in the text.

with TBA-inserted oleum-intercalated graphite. Such mixture was sonicated in DMF to give a homogeneous dispersion. The organic stability of exfoliated graphitic material enabled Langmuir–Blodgett (LB) films to be made on various transparent substrates, including glass and quartz, to produce films that are transparent and conducting. The one-, two- and three-layer LB films on quartz afforded sheet resistances of ~150, 20 and 8 kΩ at room temperature (Fig. 15) and transparencies (defined as transmittance at a wavelength of 1000 nm) of ~93, 88 and 83%, respectively (Fig. 15b and c). With a three-layer LB film, a sheet resistance of 8 kΩ can be achieved with a transparency greater than 80%.

Graphene flakes directly exfoliated from graphite using sonication and CTAB as a stabilizer have been demonstrated by Valiyaveettil and co-workers.[154] The flakes could be dispersed in common organic solvents such as DMF. Characterization of the flakes by UV-visible spectroscopy, SEM, TEM, AFM and Raman spectroscopy showed the exfoliation into

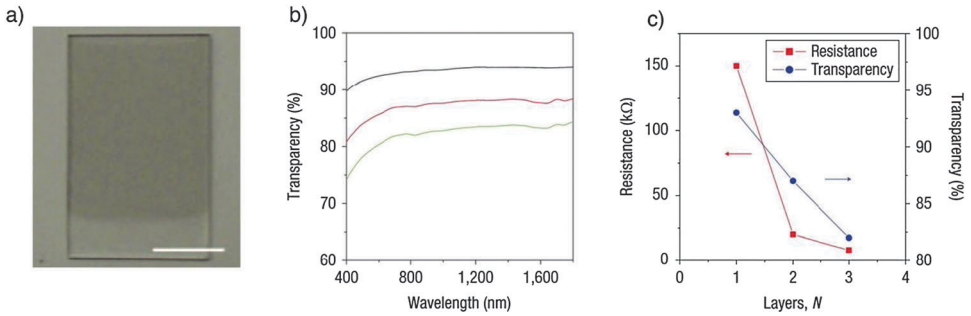

Fig. 15 Large-scale Langmuir–Blodgett (LB) film prepared from graphene sheets. (a) A photograph of a two-layer GS LB film on quartz with part of it left clear. The scale bar is 10 mm. (b) Transparency spectra of one- (black curve), two- (red curve) and three-layer (green curve) GS LB films. The transparency was defined as the transmittance at a wavelength of 1,000 nm; (c) resistances (red) and transparencies (blue) of one-, two- and three-layer LB films. Adapted from ref. 153 with permission from the Nature Publishing Group.

graphene flakes of average ~1.18 nm thickness. Field emission measurements showed a turn on voltage of 7.5 V μm^{-1} and an emission current density of 0.15 mA cm^{-2}.

Porphyrins interact with various carbon materials, such as graphite, fullerenes and carbon nanotubes (CNTs), through π-stacking that takes place between their electron-abundant aromatic cores and conjugated surfaces of the carbon materials.[155–157] Therefore, similar interactions are expected to occur between graphene and porphyrins.[158,159] To explore this idea, graphite was dispersed in solutions of porphyrins in NMP containing organic ammonium ions. The porphyrin used in this effort was 5,10,15,20-tetraphenyl-(4,11-acetylthioundecyl-oxyphenyl)-21*H*,23*H*-porphine (TATPP), which strongly interacts with the graphite surface as proven by UV-vis spectroscopy (Fig. 16a). It was found that the TATPP-assisted exfoliation of graphite can be employed to produce monolayer graphene sheets of high quality (TEM image in Fig. 16b), although statistical analysis of flake size and thickness has not been reported.

Exfoliation of graphite can also be achieved in ethanol by using quinquethiophene-terminated PEG (5TN-PEG) as a surfactant. A high electro-optical graphene film was fabricated from the graphene dispersion by vacuum filtration. After washing the surfactant with THF followed by chemical treatment with HNO_3 and $SOCl_2$, the graphene film exhibited high performance (a transmittance of 74% at 550 nm, a sheet resistance of 0.3 kΩ sq^{-1} and σ_{dc}/σ_{ac} = 3.65).

3. Polymer-assisted exfoliation

It has been recently shown that graphite can be exfoliated in water[40,128,130,160–162] and organic solvents[163,164] by using a range of conventional polymers, such as polybutadiene (PBD), polystyrene-*co*-butadiene (PBS), polystyrene (PS), polyvinylchloride (PVC), polyvinyl acetate (PVAc), polycarbonate (PC), polymethyl methacrylate (PMMA), polyvinylidenechloride (PVDC), cellulose acetate (CA),[164] ethyl cellulose (EC),[162] polyvinylpyrrolidone (PVP),[160] and even more complex systems such as water soluble pyrene-functionalized DNA,[128] which opens the door to biocompatible materials for bio-medical applications.[120]

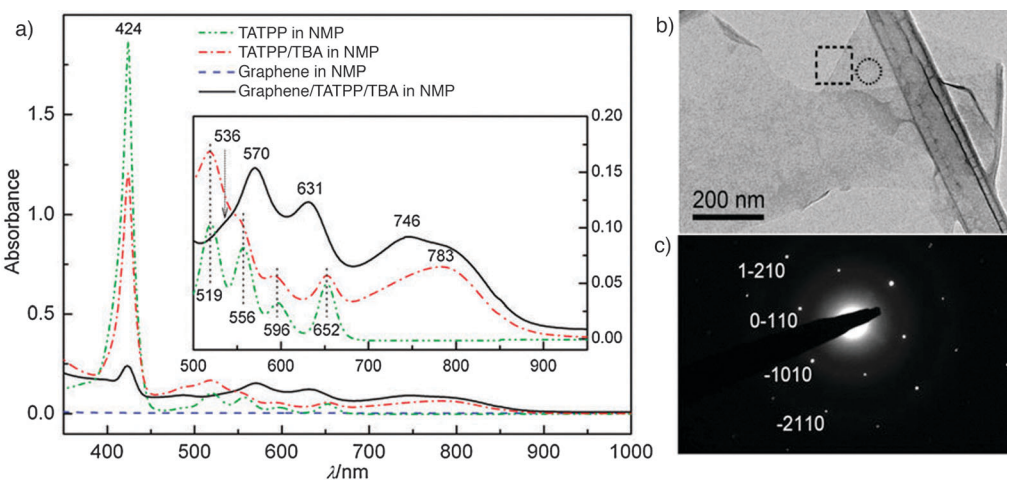

Fig. 16 (a) UV-visible spectra of graphene dispersions in 5,10,15,20-tetrakis(4,11-acetylthioundecyl-oxyphenyl)-21*H*,23*H*-porphyrin (TATPP) and tetrabutyl-ammonium hydroxide (TBA); (b) a single-layer graphene sheet visualized using a TEM; (c) electron diffraction (ED) pattern corresponding to the encircled area in panel (b). Adapted from ref. 152 with permission from the Royal Society of Chemistry.

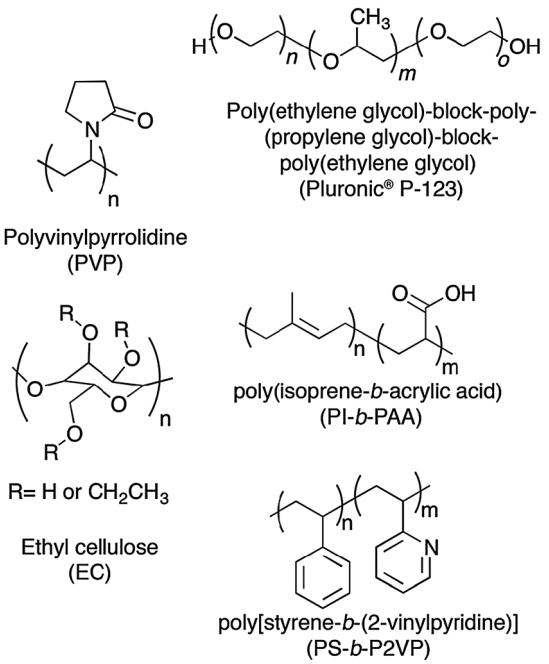

Fig. 17 Chemical structures of chosen polymers and block copolymers used as surfactants in the process of liquid-phase exfoliation of graphite towards graphene, with their names and corresponding acronyms as used in the text.

Through a modeling study, Coleman *et al.* have predicted that maximal graphene concentration can be reached when the polymer and solvent have similar Hildebrand solubility parameters as the graphene sheets.[164] Though effective, graphene concentration in the dispersions obtained therein, however, is often too low, *e.g.*, in the range of 0.006–0.022 mg mL^{-1} in THF and 0.068–0.141 mg mL^{-1} in cyclohexanone, to meet the requirements in large-scale applications. The search for a suitable polymer–solvent combination is thus important to render high quality graphene dispersions at high concentrations in conventional low-polarity, low-boiling-point organic solvents.

Graphene sheets can be exfoliated upon sonication in a variety of organic solvents such as NMP and *o*-DCB. Furthermore, exfoliated graphene in NMP can be treated with an acidic solution of poly[styrene-*b*-(2-vinylpyridine)] (PS-*b*-P2VP) or poly(isoprene-*b*-acrylic acid) (PI-*b*-PAA) block copolymers[130] (Fig. 17), resulting in aqueous solubilization of graphene. Unfortunately, the thickness of graphitic flakes amounts to 2.5 nm and 44 nm respectively, suggesting that the exfoliation protocol needs to be further optimized.

Successful production of stable high-concentration graphene dispersions in low-boiling-point, low-polarity conventional organic solvents ($CHCl_3$ and THF) was reported recently by Ye and co-workers.[163] Liquid-phase exfoliation of graphite assisted with a hyperbranched polyethylene (HBPE) as the stabilizer resulted in remarkably high-concentration (up to 0.045 mg mL^{-1} in THF and 0.18 mg mL^{-1} in chloroform) dispersions of few-layer graphene flakes. HBPE is a novel polyethylene grade synthesized through the unique ethylene chain walking polymerization technique.[165] Noteworthy, HBPE has been used recently to functionalize and solubilize multiwalled carbon nanotubes.[166] Moreover, the dispersions were further concentrated to reach graphene concentration as high as 3.4 mg mL^{-1}. Through their characterization by using TEM, AFM, and Raman spectroscopy, the majority of the graphene products was found to be high-quality, defect-free, few-layer thick graphene flakes, in particular exhibiting between 2 and 4 layer stacks and lateral dimensions in the range of 0.2–0.5 μm. Noteworthy, even after extensive washing the presence of HBPE at a significant amount was monitored by TGA, indicating its adsorption on the surface of graphene flakes.

In another investigation, a variety of ionic and non-ionic surfactants were explored by Guardia and co-workers,[161] testing their ability to aid sonication-based exfoliation and dispersion of graphene in water. Generally, non-ionic surfactants significantly outperformed their ionic counterparts (Fig. 18). The best result, a dispersion of ~1 mg mL^{-1} graphene after just 2 hours of sonication, was achieved by using the triblock copolymer Pluronic® P-123. Interestingly, an increase in sonication time to 5 hours yielded solutions in P-123 at 1.5 mg mL^{-1}, consistent with the benefits of the extended sonication time seen for exfoliation in organic solvents. It has been shown that ionic surfactants adsorb onto graphene and impart an effective charge, providing electrostatic repulsion to prevent graphene from aggregation. In the case of non-ionic surfactants, which have a hydrophobic tail and a long hydrophilic part, steric repulsions stabilize graphene. AFM analysis revealed that sheets obtained with the best surfactants had lateral sizes in the range of hundreds of nanometers, where almost all sheets were less than 5 layers thick (10–15% monolayers), consistent with other investigations of surfactant-assisted and sonication-based exfoliation.

Importantly, there is one disadvantage in using surfactants/intercalators to assist the LPE process of graphite. Regardless of whether the graphene films are prepared by drop casing or filtration, in most of the cases, the resulting material consists of graphitic flakes, surfactants, solvent or residuals from the filter, which can be problematic in the field of organic electronics. Typically, surfactants are used only to prompt the exfoliation yield, and do not possess any interesting electronic properties; however they can affect the properties of FET devices, *e.g.* by n-doping of graphene-based devices.[65] It is therefore crucial to extract graphene from post-LPE processed graphene–surfactant composites, which can be nearly impossible in the case of water-based LPE. Due to the hydrophobic nature of the graphene sheets, only the use of surfactants can complete the exfoliation of graphene in water. On the other hand, graphene–surfactant composites in organic media such as NMP or *o*-DCB should be relatively easy to process, *i.e.* to remove residual organic molecules, *e.g.* by washing the dispersions/films with the solvents capable of dissolving the molecules. Noteworthy, according to our knowledge, there has been only one report discussing this issue,[151] where the surfactant was successfully removed from graphene–surfactant films by sequential rinsing with ethanol, methanol, THF, DMSO and DMF, and chemical treatment with HNO_3 and $SOCl_2$.

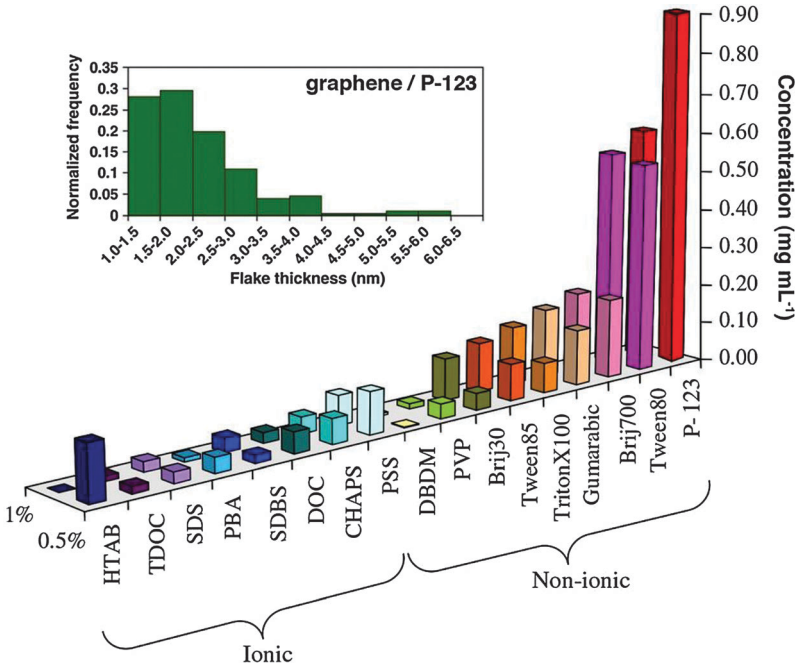

Fig. 18 Concentration of graphene in aqueous dispersions achieved by the use of different surfactants, as estimated from UV-vis absorption measurements. Two surfactant concentrations are shown: 0.5% and 1.0% wt/vol. Inset figure – histogram showing the distribution of apparent flake thickness measured by AFM on 200 objects from dispersions stabilized by the non-ionic triblock copolymer P-123. Adapted from ref. 161 with permission from Elsevier.

Nevertheless, such extraction of graphene from graphene–surfactant dispersions has to be still improved, since graphene treatment with $SOCl_2$ can result in hole doping.[151]

From the viewpoint of the final graphene concentration the use of polymers in the LPE process is undoubtedly better than the use of simple organic molecules; however, because of the strong polymer–graphene interactions the majority of graphene produced by polymer-assisted LPE of graphite cannot be extracted from graphene–polymer composites. One interesting approach relies on the use of graphene "bad solvents". Bourlinos[160] and co-workers successfully extracted graphene from the graphene–PVP mixture. To this end, the graphene was extracted from the graphene–polymer dispersion by washing it with an ethanol–chloroform mixture (both ethanol and chloroform dissolve PVP) followed by centrifugation at 4000 rpm for 10 min.

4. Conclusions & outlooks

Liquid-phase exfoliation of bulk graphite is an extremely mild, versatile and potentially up-scalable approach to obtain high-quality graphene inks using equipment available in all chemistry labs. From the chemistry point of view, the LPE in the presence of a given solvent molecule with the aid of an additional pre-designed (macro)molecule as an exfoliating agent is a path not only to increase exfoliation yield but also to avoid graphene re-aggregation due to van der Waals attraction, thereby compromising the effort made during exfoliation. Moreover, the use of the additional (macro)molecule interacting with the graphene *via* non-covalent forces makes it possible to modulate the properties of the graphene by imparting new functions to the 2D material *via* physical phenomena such as doping. From the technology point of view, the LPE approach is highly relevant as many applications rely on large-scale production using low-cost methods such as ink-jet printing and R2R. Liquid-phase exfoliation is appealing for the preparation of stable inks that can be processed in thin films and composite materials; in this regard future research is needed to control on-demand the number of layers and lateral size.

In this review, we have shown that graphene can be obtained by sonication in certain liquids. Extensive effort has been made to improve the yield and degree of exfoliation; however the yield of single-layer graphene sheets is still relatively low and requires long lasting sonication treatments. Furthermore, the material obtained has quite an amount of "waste" or by-products: because of this reason centrifugation has to be used in order to remove unexfoliated material. It will become important in the near future to define a reproducible protocol relying on the best conditions for the LPE process. This is particularly needed since to date the sonication parameters (power and time) differ from one experiment to another, *e.g.* sonication time varies from 30 min to 1000 h. While the results obtained by different research groups are very different, *e.g.* final concentration of graphene and lateral flake size, the technical factors such as sonication power are not discussed. As the potential applications of graphene multiply, it will become more and more important to be able to produce defect-free graphene in large quantities. In order to improve the exfoliation yield and reduce the by-products future effort should be devoted to the design and synthesis of new molecules

featuring an enhanced affinity for the basal plane of graphene, thereby boosting the LPE and enhancing the average size of the crystal yet retaining a good solubility in organic media such as chloroform or ethanol. Such an explorative research will pave the way towards the scaling up of LPE of graphene. Significantly, most of the knowledge generated on graphene can be applied to other layered crystals such as BN, MoS_2, WS_2, $NbSe_2$, and TaS_2[60] thereby opening novel avenues towards 2D materials exhibiting a set of new properties.

Acknowledgements

We are grateful to Vincenzo Palermo, Emanuele Treossi, Mirella El Gemayel, Markus Döbbelin, Jeffrey Mativetsky and Emanuele Orgiu for the joint research activity on graphene which was an essential source of inspiration for this review. This work was supported by the European Commission through the Marie-Curie ITN GENIUS (PITN-GA-2010-264694) and the FET project UPGRADE (project no. 309056) as well as the Agence Nationale de la Recherche through the LabEx project NIE, and the International Center for Frontier Research in Chemistry (icFRC).

References

1 K. S. Novoselov, A. K. Geim, S. V. Morozov, D. Jiang, Y. Zhang, S. V. Dubonos, I. V. Grigorieva and A. A. Firsov, *Science*, 2004, **306**, 666–669.
2 K. S. Novoselov, D. Jiang, F. Schedin, T. J. Booth, V. V. Khotkevich, S. V. Morozov and A. K. Geim, *Proc. Natl. Acad. Sci. U. S. A.*, 2005, **102**, 10451–10453.
3 A. K. Geim and K. S. Novoselov, *Nat. Mater.*, 2007, **6**, 183–191.
4 A. K. Geim, *Science*, 2009, **324**, 1530–1534.
5 C. N. R. Rao, A. K. Sood, K. S. Subrahmanyam and A. Govindaraj, *Angew. Chem., Int. Ed.*, 2009, **48**, 7752–7777.
6 M. J. Allen, V. C. Tung and R. B. Kaner, *Chem. Rev.*, 2010, **110**, 132–145.
7 D. R. Dreyer, R. S. Ruoff and C. W. Bielawski, *Angew. Chem., Int. Ed.*, 2010, **49**, 9336–9344.
8 K. S. Novoselov, V. I. Fal'ko, L. Colombo, P. R. Gellert, M. G. Schwab and K. Kim, *Nature*, 2012, **490**, 192–200.
9 C. Schafhaeutl, *J. Prakt. Chem.*, 1840, **19**, 159–174.
10 M. S. Dresselhaus and G. Dresselhaus, *Adv. Phys.*, 2002, **51**, 1–186.
11 P. R. Wallace, *Phys. Rev.*, 1947, **71**, 622–634.
12 M. Z. Cai, D. Thorpe, D. H. Adamson and H. C. Schniepp, *J. Mater. Chem.*, 2012, **22**, 24992–25002.
13 S. V. Morozov, K. S. Novoselov, M. I. Katsnelson, F. Schedin, D. C. Elias, J. A. Jaszczak and A. K. Geim, *Phys. Rev. Lett.*, 2008, **100**, 016602–016605.
14 K. I. Bolotin, K. J. Sikes, Z. Jiang, M. Klima, G. Fudenberg, J. Hone, P. Kim and H. L. Stormer, *Solid State Commun.*, 2008, **146**, 351–355.
15 X. Du, I. Skachko, A. Barker and E. Y. Andrei, *Nat. Nanotechnol.*, 2008, **3**, 491–495.
16 S. Unarunotai, Y. Murata, C. E. Chialvo, N. Mason, I. Petrov, R. G. Nuzzo, J. S. Moore and J. A. Rogers, *Adv. Mater.*, 2010, **22**, 1072–1077.
17 A. A. Balandin, *Nat. Mater.*, 2011, **10**, 569–581.
18 I. W. Frank, D. M. Tanenbaum, A. M. Van der Zande and P. L. McEuen, *J. Vac. Sci. Technol., B*, 2007, **25**, 2558–2561.
19 R. Faccio, P. A. Denis, H. Pardo, C. Goyenola and A. W. Mombru, *J. Phys.: Condens. Matter*, 2009, **21**, 285304–285310.
20 F. Scarpa, S. Adhikari and A. S. Phani, *Nanotechnology*, 2009, **20**, 065709.
21 H. K. Chae, D. Y. Siberio-Perez, J. Kim, Y. Go, M. Eddaoudi, A. J. Matzger, M. O'Keeffe and O. M. Yaghi, *Nature*, 2004, **427**, 523–527.
22 M. D. Stoller, S. J. Park, Y. W. Zhu, J. H. An and R. S. Ruoff, *Nano Lett.*, 2008, **8**, 3498–3502.
23 S. Patchkovskii, J. S. Tse, S. N. Yurchenko, L. Zhechkov, T. Heine and G. Seifert, *Proc. Natl. Acad. Sci. U. S. A.*, 2005, **102**, 10439–10444.
24 F. Schedin, A. K. Geim, S. V. Morozov, E. W. Hill, P. Blake, M. I. Katsnelson and K. S. Novoselov, *Nat. Mater.*, 2007, **6**, 652–655.
25 V. Dua, S. P. Surwade, S. Ammu, S. R. Agnihotra, S. Jain, K. E. Roberts, S. Park, R. S. Ruoff and S. K. Manohar, *Angew. Chem., Int. Ed.*, 2010, **49**, 2154–2157.
26 P. Avouris, Z. H. Chen and V. Perebeinos, *Nat. Nanotechnol.*, 2007, **2**, 605–615.
27 J. S. Wu, W. Pisula and K. Müllen, *Chem. Rev.*, 2007, **107**, 718–747.
28 K. Müllen and J. P. Rabe, *Acc. Chem. Res.*, 2008, **41**, 511–520.
29 G. Eda and M. Chhowalla, *Nano Lett.*, 2009, **9**, 814–818.
30 G. M. Scheuermann, L. Rumi, P. Steurer, W. Bannwarth and R. Mülhaupt, *J. Am. Chem. Soc.*, 2009, **131**, 8262–8270.
31 W. R. Yang, K. R. Ratinac, S. P. Ringer, P. Thordarson, J. J. Gooding and F. Braet, *Angew. Chem., Int. Ed.*, 2010, **49**, 2114–2138.
32 J. S. Bunch, S. S. Verbridge, J. S. Alden, A. M. van der Zande, J. M. Parpia, H. G. Craighead and P. L. McEuen, *Nano Lett.*, 2008, **8**, 2458–2462.
33 X. Wang, L. J. Zhi and K. Müllen, *Nano Lett.*, 2008, **8**, 323–327.
34 J. B. Wu, M. Agrawal, H. A. Becerril, Z. N. Bao, Z. F. Liu, Y. S. Chen and P. Peumans, *ACS Nano*, 2010, **4**, 43–48.
35 S. Bae, H. Kim, Y. Lee, X. F. Xu, J. S. Park, Y. Zheng, J. Balakrishnan, T. Lei, H. R. Kim, Y. I. Song, Y. J. Kim, K. S. Kim, B. Ozyilmaz, J. H. Ahn, B. H. Hong and S. Iijima, *Nat. Nanotechnol.*, 2010, **5**, 574–578.
36 F. N. Xia, T. Mueller, Y. M. Lin, A. Valdes-Garcia and P. Avouris, *Nat. Nanotechnol.*, 2009, **4**, 839–843.
37 T. Mueller, F. N. A. Xia and P. Avouris, *Nat. Photonics*, 2010, **4**, 297–301.
38 T. J. Echtermeyer, L. Britnell, P. K. Jasnos, A. Lombardo, R. V. Gorbachev, A. N. Grigorenko, A. K. Geim, A. C. Ferrari and K. S. Novoselov, *Nat. Commun.*, 2011, **2**, 458–462.
39 G. Konstantatos, M. Badioli, L. Gaudreau, J. Osmond, M. Bernechea, F. P. G. de Arquer, F. Gatti and F. H. L. Koppens, *Nat. Nanotechnol.*, 2012, **7**, 363–368.

40 T. Hasan, F. Torrisi, Z. Sun, D. Popa, V. Nicolosi, G. Privitera, F. Bonaccorso and A. C. Ferrari, *Phys. Status Solidi B*, 2010, **247**, 2953–2957.
41 Z. P. Sun, T. Hasan, F. Torrisi, D. Popa, G. Privitera, F. Q. Wang, F. Bonaccorso, D. M. Basko and A. C. Ferrari, *ACS Nano*, 2010, **4**, 803–810.
42 E. W. Hill, A. K. Geim, K. Novoselov, F. Schedin and P. Blake, *IEEE Trans. Magn.*, 2006, **42**, 2694–2696.
43 N. Tombros, C. Jozsa, M. Popinciuc, H. T. Jonkman and B. J. van Wees, *Nature*, 2007, **448**, 571–574.
44 K. S. Kim, Y. Zhao, H. Jang, S. Y. Lee, J. M. Kim, K. S. Kim, J. H. Ahn, P. Kim, J. Y. Choi and B. H. Hong, *Nature*, 2009, **457**, 706–710.
45 X. S. Li, W. W. Cai, J. H. An, S. Kim, J. Nah, D. X. Yang, R. Piner, A. Velamakanni, I. Jung, E. Tutuc, S. K. Banerjee, L. Colombo and R. S. Ruoff, *Science*, 2009, **324**, 1312–1314.
46 C. Berger, Z. M. Song, X. B. Li, X. S. Wu, N. Brown, C. Naud, D. Mayou, T. B. Li, J. Hass, A. N. Marchenkov, E. H. Conrad, P. N. First and W. A. de Heer, *Science*, 2006, **312**, 1191–1196.
47 L. Chen, Y. Hernandez, X. L. Feng and K. Müllen, *Angew. Chem., Int. Ed.*, 2012, **51**, 7640–7654.
48 C.-A. Palma and P. Samorì, *Nat. Chem.*, 2011, **3**, 431–436.
49 V. León, M. Quintana, M. A. Herrero, J. L. G. Fierro, A. de la Hoz, M. Prato and E. Vázquez, *Chem. Commun.*, 2011, **47**, 10936–10938.
50 J. N. Coleman, *Adv. Funct. Mater.*, 2009, **19**, 3680–3695.
51 J. N. Coleman, *Acc. Chem. Res.*, 2013, **46**, 14–22.
52 M. Quintana, K. Spyrou, M. Grzelczak, W. R. Browne, P. Rudolf and M. Prato, *ACS Nano*, 2010, **4**, 3527–3533.
53 F. Bonaccorso, A. Lombardo, T. Hasan, Z. P. Sun, L. Colombo and A. C. Ferrari, *Mater. Today*, 2012, **15**, 564–589.
54 B. C. Brodie, *Ann. Chim. Phys.*, 1860, **59**, 466–472.
55 L. Staudenmaier, *Ber. Dtsch. Chem. Ges.*, 1898, **31**, 1481–1499.
56 W. S. Hummers and R. E. Offeman, *J. Am. Chem. Soc.*, 1958, **80**, 1339.
57 E. Treossi, M. Melucci, A. Liscio, M. Gazzano, P. Samorì and V. Palermo, *J. Am. Chem. Soc.*, 2009, **131**, 15576–15577.
58 A. Liscio, G. P. Veronese, E. Treossi, F. Suriano, F. Rossella, V. Bellani, R. Rizzoli, P. Samorì and V. Palermo, *J. Mater. Chem.*, 2011, **21**, 2924–2931.
59 M. Melucci, E. Treossi, L. Ortolani, G. Giambastiani, V. Morandi, P. Klar, C. Casiraghi, P. Samorì and V. Palermo, *J. Mater. Chem.*, 2010, **20**, 9052–9060.
60 V. Nicolosi, M. Chhowalla, M. G. Kanatzidis, M. S. Strano and J. N. Coleman, *Science*, 2013, **340**, 1226419, DOI: 10.1126/science.1226419.
61 J. N. Coleman, M. Lotya, A. O'Neill, S. D. Bergin, P. J. King, U. Khan, K. Young, A. Gaucher, S. De, R. J. Smith, I. V. Shvets, S. K. Arora, G. Stanton, H. Y. Kim, K. Lee, G. T. Kim, G. S. Duesberg, T. Hallam, J. J. Boland, J. J. Wang, J. F. Donegan, J. C. Grunlan, G. Moriarty, A. Shmeliov, R. J. Nicholls, J. M. Perkins, E. M. Grieveson, K. Theuwissen, D. W. McComb, P. D. Nellist and V. Nicolosi, *Science*, 2011, **331**, 568–571.
62 T. Svedberg and K. O. Pedersen, *The Ultracentrifuge*, Oxford, 1940.
63 W. Qian, R. Hao, Y. L. Hou, Y. Tian, C. M. Shen, H. J. Gao and X. L. Liang, *Nano Res.*, 2009, **2**, 706–712.
64 F. Torrisi, T. Hasan, W. P. Wu, Z. P. Sun, A. Lombardo, T. S. Kulmala, G. W. Hsieh, S. J. Jung, F. Bonaccorso, P. J. Paul, D. P. Chu and A. C. Ferrari, *ACS Nano*, 2012, **6**, 2992–3006.
65 B. Li, A. V. Klekachev, M. Cantoro, C. Huyghebaert, A. Stesmans, I. Asselberghs, S. De Gendt and S. De Feyter, *Nanoscale*, 2013, DOI: 10.1039/c1033nr01255g.
66 S. Stankovich, D. A. Dikin, R. D. Piner, K. A. Kohlhaas, A. Kleinhammes, Y. Jia, Y. Wu, S. T. Nguyen and R. S. Ruoff, *Carbon*, 2007, **45**, 1558–1565.
67 I. Jung, D. A. Dikin, R. D. Piner and R. S. Ruoff, *Nano Lett.*, 2008, **8**, 4283–4287.
68 S. Park, J. H. An, I. W. Jung, R. D. Piner, S. J. An, X. S. Li, A. Velamakanni and R. S. Ruoff, *Nano Lett.*, 2009, **9**, 1593–1597.
69 J. M. Mativetsky, A. Liscio, E. Treossi, E. Orgiu, A. Zanelli, P. Samorì and V. Palermo, *J. Am. Chem. Soc.*, 2011, **133**, 14320–14326.
70 F. J. Tölle, M. Fabritius and R. Mülhaupt, *Adv. Funct. Mater.*, 2012, **22**, 1136–1144.
71 C. Gomez-Navarro, R. T. Weitz, A. M. Bittner, M. Scolari, A. Mews, M. Burghard and K. Kern, *Nano Lett.*, 2007, **7**, 3499–3503.
72 G. Eda, G. Fanchini and M. Chhowalla, *Nat. Nanotechnol.*, 2008, **3**, 270–274.
73 K. N. Kudin, B. Ozbas, H. C. Schniepp, R. K. Prud'homme, I. A. Aksay and R. Car, *Nano Lett.*, 2008, **8**, 36–41.
74 H. Kang, A. Kulkarni, S. Stankovich, R. S. Ruoff and S. Baik, *Carbon*, 2009, **47**, 1520–1525.
75 D. Yang, A. Velamakanni, G. Bozoklu, S. Park, M. Stoller, R. D. Piner, S. Stankovich, I. Jung, D. A. Field, C. A. Ventrice and R. S. Ruoff, *Carbon*, 2009, **47**, 145–152.
76 Y. Hernandez, V. Nicolosi, M. Lotya, F. M. Blighe, Z. Sun, S. De, I. T. McGovern, B. Holland, M. Byrne, Y. K. Gun'Ko, J. J. Boland, P. Niraj, G. Duesberg, S. Krishnamurthy, R. Goodhue, J. Hutchison, V. Scardaci, A. C. Ferrari and J. N. Coleman, *Nat. Nanotechnol.*, 2008, **3**, 563–568.
77 A. B. Bourlinos, V. Georgakilas, R. Zboril, T. A. Steriotis and A. K. Stubos, *Small*, 2009, **5**, 1841–1845.
78 C. E. Hamilton, J. R. Lomeda, Z. Z. Sun, J. M. Tour and A. R. Barron, *Nano Lett.*, 2009, **9**, 3460–3462.
79 U. Khan, A. O'Neill, M. Lotya, S. De and J. N. Coleman, *Small*, 2010, **6**, 864–871.
80 X. Y. Zhang, A. C. Coleman, N. Katsonis, W. R. Browne, B. J. van Wees and B. L. Feringa, *Chem. Commun.*, 2010, **46**, 7539–7541.
81 D. Nuvoli, L. Valentini, V. Alzari, S. Scognamillo, S. B. Bon, M. Piccinini, J. Illescas and A. Mariani, *J. Mater. Chem.*, 2011, **21**, 3428–3431.
82 A. O'Neill, U. Khan, P. N. Nirmalraj, J. Boland and J. N. Coleman, *J. Phys. Chem. C*, 2011, **115**, 5422–5428.
83 U. Khan, H. Porwal, A. O'Neill, K. Nawaz, P. May and J. N. Coleman, *Langmuir*, 2011, **27**, 9077–9082.

84 U. Khan, A. O'Neill, H. Porwal, P. May, K. Nawaz and J. N. Coleman, *Carbon*, 2012, **50**, 470–475.
85 T. J. Mason and J. Phillip, *Applied Sonochemistry*, Wiley-VCH, Weinheim, 2002.
86 J. N. Israelachvili, *Intermolecular and surface forces*, Academic press, revised 3rd edn, 2011.
87 A. C. Ferrari, J. C. Meyer, V. Scardaci, C. Casiraghi, M. Lazzeri, F. Mauri, S. Piscanec, D. Jiang, K. S. Novoselov, S. Roth and A. K. Geim, *Phys. Rev. Lett.*, 2006, **97**, 187401.
88 C. Valles, C. Drummond, H. Saadaoui, C. A. Furtado, M. He, O. Roubeau, L. Ortolani, M. Monthioux and A. Penicaud, *J. Am. Chem. Soc.*, 2008, **130**, 15802–15804.
89 J. C. Meyer, A. K. Geim, M. I. Katsnelson, K. S. Novoselov, T. J. Booth and S. Roth, *Nature*, 2007, **446**, 60–63.
90 C. Casiraghi, A. Hartschuh, E. Lidorikis, H. Qian, H. Harutyunyan, T. Gokus, K. S. Novoselov and A. C. Ferrari, *Nano Lett.*, 2007, **7**, 2711–2717.
91 P. Blake, E. W. Hill, A. H. C. Neto, K. S. Novoselov, D. Jiang, R. Yang, T. J. Booth and A. K. Geim, *Appl. Phys. Lett.*, 2007, **91**, 063124.
92 C. Casiraghi, in*Spectroscopic Properties of Inorganic and Organometallic Compounds: Techniques, Materials and Applications*, The Royal Society of Chemistry, 2012, vol. 43, pp. 29–56.
93 A. C. Ferrari and D. M. Basko, *Nat. Nanotechnol.*, 2013, **8**, 235–246.
94 A. C. Ferrari, *Solid State Commun.*, 2007, **143**, 47–57.
95 J. Yan, Y. B. Zhang, P. Kim and A. Pinczuk, *Phys. Rev. Lett.*, 2007, **98**, 166802–166805.
96 A. Das, S. Pisana, B. Chakraborty, S. Piscanec, S. K. Saha, U. V. Waghmare, K. S. Novoselov, H. R. Krishnamurthy, A. K. Geim, A. C. Ferrari and A. K. Sood, *Nat. Nanotechnol.*, 2008, **3**, 210–215.
97 A. Das, B. Chakraborty, S. Piscanec, S. Pisana, A. K. Sood and A. C. Ferrari, *Phys. Rev. B: Condens. Matter Mater. Phys.*, 2009, **79**, 155417–155423.
98 M. Kalbac, A. Reina-Cecco, H. Farhat, J. Kong, L. Kavan and M. S. Dresselhaus, *ACS Nano*, 2010, **4**, 6055–6063.
99 C. F. Chen, C. H. Park, B. W. Boudouris, J. Horng, B. S. Geng, C. Girit, A. Zettl, M. F. Crommie, R. A. Segalman, S. G. Louie and F. Wang, *Nature*, 2011, **471**, 617–620.
100 W. J. Zhao, P. H. Tan, J. Liu and A. C. Ferrari, *J. Am. Chem. Soc.*, 2011, **133**, 5941–5946.
101 Y. M. You, Z. H. Ni, T. Yu and Z. X. Shen, *Appl. Phys. Lett.*, 2008, **93**, 163112–163115.
102 D. M. Basko, *Phys. Rev. B: Condens. Matter Mater. Phys.*, 2009, **79**, 205428.
103 C. Casiraghi, A. Hartschuh, H. Qian, S. Piscanec, C. Georgi, A. Fasoli, K. S. Novoselov, D. M. Basko and A. C. Ferrari, *Nano Lett.*, 2009, **9**, 1433–1441.
104 A. K. Gupta, T. J. Russin, H. R. Gutierrez and P. C. Eklund, *ACS Nano*, 2009, **3**, 45–52.
105 C. X. Cong, T. Yu and H. M. Wang, *ACS Nano*, 2010, **4**, 3175–3180.
106 T. Gokus, R. R. Nair, A. Bonetti, M. Bohmler, A. Lombardo, K. S. Novoselov, A. K. Geim, A. C. Ferrari and A. Hartschuh, *ACS Nano*, 2009, **3**, 3963–3968.
107 J. H. Chen, W. G. Cullen, C. Jang, M. S. Fuhrer and E. D. Williams, *Phys. Rev. Lett.*, 2009, **102**, 236805–236808.
108 Z. H. Ni, L. A. Ponomarenko, R. R. Nair, R. Yang, S. Anissimova, I. V. Grigorieva, F. Schedin, P. Blake, Z. X. Shen, E. H. Hill, K. S. Novoselov and A. K. Geim, *Nano Lett.*, 2010, **10**, 3868–3872.
109 B. C. Brodie, *Philos. Trans. R. Soc. London*, 1859, **149**, 249–259.
110 H. P. Boehm, A. Clauss, G. O. Fisher and U. Z. Hofmann, *Z. Anorg. Allg. Chem.*, 1962, **316**, 119–127.
111 H. P. Boehm and W. Z. Scholtz, *Z. Anorg. Allg. Chem.*, 1965, **335**, 74–79.
112 W. S. Hummers and R. E. Offeman, *J. Am. Chem. Soc.*, 1958, **80**, 1339.
113 L. Staudenmaier, *Ber. Dtsch. Chem. Ges.*, 1898, **31**, 1481–1487.
114 H. M. Solomon, B. A. Burgess, G. L. Kennedy and R. E. Staples, *Drug Chem. Toxicol.*, 1995, **18**, 271–293.
115 G. L. Kennedy and H. Sherman, *Drug Chem. Toxicol.*, 1986, **9**, 147–170.
116 F. Hennrich, R. Krupke, K. Arnold, J. A. R. Stutz, S. Lebedkin, T. Koch, T. Schimmel and M. M. Kappes, *J. Phys. Chem. B*, 2007, **111**, 1932–1937.
117 M. Lotya, Y. Hernandez, P. J. King, R. J. Smith, V. Nicolosi, L. S. Karlsson, F. M. Blighe, S. De, Z. M. Wang, I. T. McGovern, G. S. Duesberg and J. N. Coleman, *J. Am. Chem. Soc.*, 2009, **131**, 3611–3620.
118 M. K. Brakke, *Arch. Biochem. Biophys.*, 1953, **45**, 275–290.
119 L. Gong, I. A. Kinloch, R. J. Young, I. Riaz, R. Jalil and K. S. Novoselov, *Adv. Mater.*, 2010, **22**, 2694–2697.
120 A. Bianco, *Angew. Chem., Int. Ed.*, 2013, **52**, 4986–4997.
121 X. Dong, Y. Shi, Y. Zhao, D. Chen, J. Ye, Y. Yao, F. Gao, Z. Ni, T. Yu and Z. Shen, *Phys. Rev. Lett.*, 2009, **102**, 135501.
122 J. M. Englert, J. Rohrl, C. D. Schmidt, R. Graupner, M. Hundhausen, F. Hauke and A. Hirsch, *Adv. Mater.*, 2009, **21**, 4265–4269.
123 Q. Su, S. P. Pang, V. Alijani, C. Li, X. L. Feng and K. Müllen, *Adv. Mater.*, 2009, **21**, 3191–3195.
124 S. Bose, T. Kuila, A. K. Mishra, N. H. Kim and J. H. Lee, *Nanotechnology*, 2011, **22**, 1–7.
125 A. Ghosh, K. V. Rao, S. J. George and C. N. R. Rao, *Chem.–Eur. J.*, 2010, **16**, 2700–2704.
126 J.-H. Jang, D. Rangappa, Y.-U. Kwon and I. Honma, *J. Mater. Chem.*, 2010, **21**, 3462–3466.
127 D. W. Lee, T. Kim and M. Lee, *Chem. Commun.*, 2011, **47**, 8259–8261.
128 F. Liu, J. Y. Choi and T. S. Seo, *Chem. Commun.*, 2010, **46**, 2844–2846.
129 M. Lotya, P. J. King, U. Khan, S. De and J. N. Coleman, *ACS Nano*, 2010, **4**, 3155–3162.
130 T. Skaltsas, N. Karousis, H. Yan, C.-R. Wang, S. Pispas and N. Tagmatarchis, *J. Mater. Chem.*, 2012, 21507–21512.
131 H. Zhang, J. Q. Wen, X. P. Meng, Y. D. Yao, G. F. Yin, X. M. Liao and Z. B. Huang, *Chem. Lett.*, 2012, **41**, 747–749.
132 M. Zhang, R. R. Parajuli, D. Mastrogiovanni, B. Dai, P. Lo, W. Cheung, R. Brukh, P. L. Chiu, T. Zhou, Z. F. Liu, E. Garfunkel and H. X. He, *Small*, 2010, **6**, 1100–1107.

133 H. Yang, Y. Hernandez, A. Schlierf, A. Felten, A. Eckmann, S. Johal, P. Louette, J. J. Pireaux, X. Feng, K. Müllen, V. Palermo and C. Casiraghi, *Carbon*, 2013, **53**, 357–365.

134 D. Parviz, S. Das, H. S. T. Ahmed, F. Irin, S. Bhattacharia and M. J. Green, *ACS Nano*, 2012, **6**, 8857–8867.

135 A. Schlierf, H. Yang, E. Gebremedhn, E. Treossi, L. Ortolani, L. Chen, A. Minoia, V. Morandi, P. Samorì, C. Casiraghi, D. Beljonne and V. Palermo, *Nanoscale*, 2013, **5**, 4205–4216.

136 S. Sampath, A. N. Basuray, K. J. Hartlieb, T. Aytun, S. I. Stupp and J. F. Stoddart, *Adv. Mater.*, 2013, **25**, 2740–2745.

137 B. Schmaltz, T. Weil and K. Müllen, *Adv. Mater.*, 2009, **21**, 1067–1078.

138 R. Rieger and K. Müllen, *J. Phys. Org. Chem.*, 2010, **23**, 315–325.

139 C. Li, M. Y. Liu, N. G. Pschirer, M. Baumgarten and K. Müllen, *Chem. Rev.*, 2010, **110**, 6817–6855.

140 T. M. Figueira-Duarte and K. Müllen, *Chem. Rev.*, 2011, **111**, 7260–7314.

141 X. L. Feng, V. Marcon, W. Pisula, M. R. Hansen, J. Kirkpatrick, F. Grozema, D. Andrienko, K. Kremer and K. Müllen, *Nat. Mater.*, 2009, **8**, 421–426.

142 Z. J. Chen, A. Lohr, C. R. Saha-Moller and F. Wurthner, *Chem. Soc. Rev.*, 2009, **38**, 564–584.

143 J. Björk, F. Hanke, C.-A. Palma, P. Samorì, M. Cecchini and M. Persson, *J. Phys. Chem. Lett.*, 2010, **1**, 3407–3412.

144 T. Fujigaya and N. Nakashima, *Polym. J.*, 2008, **40**, 577–589.

145 M. Zhang, R. R. Parajuli, D. Mastrogiovanni, B. Dai, P. Lo, W. Cheung, R. Brukh, P. L. Chiu, T. Zhou and Z. Liu, *Small*, 2010, **6**, 1100–1107.

146 Y. X. Xu, H. Bai, G. W. Lu, C. Li and G. Q. Shi, *J. Am. Chem. Soc.*, 2008, **130**, 5856–5857.

147 C. D. Schmidt, C. Boettcher and A. Hirsch, *Eur. J. Org. Chem.*, 2007, 5497–5505.

148 R. Hao, W. Qian, L. H. Zhang and Y. L. Hou, *Chem. Commun.*, 2008, 6576–6578.

149 S. De, P. J. King, M. Lotya, A. O'Neill, E. M. Doherty, Y. Hernandez, G. S. Duesberg and J. N. Coleman, *Small*, 2010, **6**, 458–464.

150 L. L. Chua, J. Zaumseil, J. F. Chang, E. C. W. Ou, P. K. H. Ho, H. Sirringhaus and R. H. Friend, *Nature*, 2005, **434**, 194–199.

151 M. S. Kang, K. T. Kim, J. U. Lee and W. H. Jo, *J. Mater. Chem. C*, 2013, **1**, 1870–1875.

152 J. Geng, B. S. Kong, S. B. Yang and H. T. Jung, *Chem. Commun.*, 2010, **46**, 5091–5093.

153 X. Li, G. Zhang, X. Bai, X. Sun, X. Wang, E. Wang and H. Dai, *Nat. Nanotechnol.*, 2008, **3**, 538–542.

154 S. Vadukumpully, J. Paul and S. Valiyaveettil, *Carbon*, 2009, **47**, 3288–3294.

155 J. Otsuki, E. Nagamine, T. Kondo, K. Iwasaki, M. Asakawa and K. Miyake, *J. Am. Chem. Soc.*, 2005, **127**, 10400–10405.

156 T. Hasobe, H. Imahori, P. V. Kamat, T. K. Ahn, S. K. Kim, D. Kim, A. Fujimoto, T. Hirakawa and S. Fukuzumi, *J. Am. Chem. Soc.*, 2005, **127**, 1216–1228.

157 J. X. Geng, Y. K. Ko, S. C. Youn, Y. H. Kim, S. A. Kim, D. H. Jung and H. T. Jung, *J. Phys. Chem. C*, 2008, **112**, 12264–12271.

158 J. Malig, A. W. I. Stephenson, P. Wagner, G. G. Wallace, D. L. Officer and D. M. Guldi, *Chem. Commun.*, 2012, **48**, 8745–8747.

159 L. Brinkhaus, G. Katsukis, J. Malig, R. D. Costa, M. Garcia-Iglesias, P. Vázquez, T. Torres and D. M. Guldi, *Small*, 2013, **9**, 2348–2357, DOI: 10.1002/smll.201202427.

160 A. B. Bourlinos, V. Georgakilas, R. Zboril, T. A. Steriotis, A. K. Stubos and C. Trapalis, *Solid State Commun.*, 2009, **149**, 2172–2176.

161 L. Guardia, M. J. Fernandez-Merino, J. I. Paredes, P. Solis-Fernandez, S. Villar-Rodil, A. Martinez-Alonso and J. M. D. Tascon, *Carbon*, 2011, **49**, 1653–1662.

162 Y. T. Liang and M. C. Hersam, *J. Am. Chem. Soc.*, 2010, **132**, 17661–17663.

163 L. Xu, J.-W. McGraw, F. Gao, M. Grundy, Z. Ye, Z. Gu and J. L. Shepherd, *J. Phys. Chem. C*, 2013, **117**, 10730–10742.

164 P. May, U. Khan, J. M. Hughes and J. N. Coleman, *J. Phys. Chem. C*, 2012, **116**, 11393–11400.

165 Z. B. Ye and S. Y. Li, *Macromol. React. Eng.*, 2010, **4**, 319–332.

166 L. X. Xu, Z. B. Ye, Q. Z. Cui and Z. Y. Gu, *Macromol. Chem. Phys.*, 2009, **210**, 2194–2202.

